

CNDO/2 CALCULATIONS ON LOW-LYING ELECTRONIC STATES

OF ACETONE AND FORMALDEHYDE

**CNDO/2 CALCULATIONS  
ON LOW-LYING  
ELECTRONIC STATES  
OF ACETONE AND FORMALDEHYDE**

**By**

**GERALD WHITE, B.Sc.**

**A Thesis**

**Submitted to the School of Graduate Studies  
in Partial Fulfilment of the Requirements  
for the Degree  
Master of Science**

**McMaster University**

**September, 1971**

MASTER OF SCIENCE (1970)  
(Chemistry)

McMASTER UNIVERSITY  
Hamilton, Ontario.

TITLE: CNDO/2 Calculations on Low-Lying Electronic States of Acetone  
and Formaldehyde.

AUTHOR: Gerald White, B.Sc. (Loyola University of Montreal).

SUPERVISOR: Professor A. J. Yarwood.

NUMBER OF PAGES: vii, 103

SCOPE AND CONTENTS:

Various low-lying electronic states of formaldehyde and acetone have been investigated, using molecular orbital calculations, to determine their involvement in the photochemical system. The potential energy surfaces of these states were calculated using the CNDO/2.

The results of this study show that the decomposition of formaldehyde to molecular products  $H_2$  and CO (process II) occurs via the ground state; the potential surface of this process was studied using configuration interaction methods.

The process leading to radical products in both acetone and formaldehyde (process I) can arise either directly from the singlet and triplet ( $n, \pi^*$ ) states via a reaction path of no symmetry, or by crossing to the  $^3(\pi, \pi^*)$  state should  $C_s$  symmetry be maintained. The ground state is the only other state correlating with radical products.

## ACKNOWLEDGEMENTS

I would like to express my gratitude to my research director, Dr. A. J. Yarwood, for his suggestions, advice and encouragement, without which this work would have been impossible.

I would like to express my appreciation to Dr. D. P. Santry for his instruction in the use of the CNDO/2 programmes, which he supplied for this study, and many helpful suggestions.

I also wish to thank Mr. Séamus O'Shea, Dr. Raymond Gangi, Dr. James Bacon, Dr. Hari Samant and Dr. Anthony Jackson for many stimulating discussions and helpful suggestions.

I wish also to express thanks to those who took part in the typing of this thesis: Mrs. Hanna Lindemann; Miss Diane Allen; Miss Veronica Komczynski; and, particularly, Miss Jan Iverson, who is able to decipher my handwriting.

I particularly wish to thank my wife for giving me encouragement and showing much tolerance in putting up with me during the course of this work.

Finally, a word of thanks to the many who, while perhaps extending my stay a trifle, made it interesting and enjoyable.

## TABLE OF CONTENTS

<u>Chapter</u>	<u>Title</u>	<u>Page</u>
	<b>Introduction</b>	
I	<b>An Introduction to Molecular Orbital Theory.</b>	1
	<b>The Formaldehyde Photochemical System</b>	
II	<b>A Review of Experimental Information.</b>	19
III	<b>The Calculations on the Formaldehyde System.</b>	33
IV	<b>Suggestions for Further Experiments.</b>	70
	<b>The Acetone Photochemical System</b>	
V	<b>A Review of Experimental Information.</b>	73
VI	<b>Calculations on the Acetone System.</b>	81
	<b>Conclusion</b>	
VII	<b>Discussion</b>	93
	<b>References</b>	95
	<b>Appendix</b>	99

LIST OF TABLES

<u>Table</u>	<u>Title</u>	<u>Page</u>
I	The Matrix Elements of the Interaction Matrix: Off Diagonal Elements.	18
II	A Comparison of Observed and Calculated Geometries of H <sub>2</sub> CO.	34
III	A Comparison of Calculated with Observed Transition Energies of H <sub>2</sub> CO.	35
IV	Transition Energies: A Comparison of Various Cal- culations of the Transition Energies.	40
V	Energies of Decomposition Products of H <sub>2</sub> CO <sup>1</sup> (n <sup>2</sup> ,σ* <sup>2</sup> ).	43
VI	Equilibrium Geometries and Transition Energies of Two States of HCO.	58
VII	Kinetic Data on Acetone by Larson and O'Neal.	77
VIII	Equilibrium Geometries of Various Electronic States of Acetone.	83
IX	The Equilibrium Geometries of Two States of Acetyl Radical.	86
X	The Equilibrium Geometries for Values of R <sub>3</sub> (C-C) of 1.7 Å and 2.75 Å.	90
XI	The Eigenvectors of Formaldehyde in the Ground State at Equilibrium Geometry.	100
XII	The Eigenvectors of Acetone in the Ground State at Equilibrium Geometry.	101

## LIST OF FIGURES

<u>Figure</u>	<u>Title</u>	<u>Page</u>
I	The Allowed Transitions in the $C_{2v}$ Point Group.	23
II	The Normal Vibrational Modes of Formaldehyde.	24
III	The Coordinate System of Formaldehyde.	26
IV	Variation of the Out of Plane Angle, $P_s$ , in the $^1_{n,\pi^*}$ State.	37
V	The Energy of $H_2$ vs. Bond Length (Ground State).	44
VI	The Energy of CO vs. Bond Length (Ground State).	45
VII	The Energy of $H_2CO$ vs. Theta: $n^2, \sigma^{*2}$ State.	46
VIII	The Energy of $H_2CO$ vs. Theta: $n^2, \sigma^{*2}$ State.	47
IX	The Energy of $H_2CO$ vs. Theta: $n^2, \sigma^{*2}$ State.	48
X	The Energy of $H_2CO$ vs. Theta: $n^2, \sigma^{*2}$ State.	49
XI	Potential Energy Surface for Ground State Formaldehyde: Part A.	52
XII	Potential Energy Surface for Ground State Formaldehyde: Part B.	53
XIII	The Correlation of States of $H_2CO$ and $(CH_3)_2CO$ with Radical Products.	61
XIV	The Energy of $HCO + H$ (Ground State) as a Function of Theta 2.	63
XV	The Energy of $HCO + H$ (Ground State) as a Function of Theta 2.	64

<u>Figure</u>	<u>Title</u>	<u>Page</u>
XVI	The Coordinates Varied in the Calculations on Acetone.	84
XVII	Variation of the Energy of an Acetyl Radical with a Methyl Radical.	88
XVIII	Variation of the Energy of an Acetyl Radical with a Methyl Radical.	89



## INTRODUCTION

### Chapter I

#### An Introduction to Molecular Orbital Theory

Considerable interest has been shown in the photochemical systems of formaldehyde, acetone, and other simple carbonyl compounds<sup>1,2</sup>. These molecules are particularly useful for the investigation of the primary chemical and physical processes occurring upon the absorption of light. These molecules have reasonably well defined spectra, undergo fluorescence or phosphorescence, and the products of the photolysis are few in number and are uncomplicated.

From a theoretical standpoint, the investigation of the electronic states involved in the photochemical system of formaldehyde and acetone is made practical by their small size. It is expected that a study of the excited states and the potential energy surfaces will aid in the interpretation of the data collected from studies of these molecules. It will also be useful in the elucidation of the primary processes undergone by photoexcited carbonyl compounds.

#### Hartree-Fock Theory<sup>3,4</sup>

A molecule, in general, may be considered as constructed of a group of nuclei, the atomic nuclei from which the molecule is constructed, which move, relative to each other, about a constant centre of gravity. About these nuclei move a number of electrons. The motion of the electrons and nuclei is described by a wavefunction, such that:

$$HY = EY$$

E: The total energy of the system

H: The total energy operator, called the

Hamiltonian Operator, and is described:

$$H(x, X) = -\sum_A \frac{\hbar^2}{8\pi^2 M_A} \nabla_A^2 - \sum_P \frac{\hbar^2}{8\pi^2 M} \nabla_P^2 \} - \sum_A \frac{\hbar^2 \nabla_A^2}{8\pi^2 M_A} - \sum_P \frac{\hbar^2 \nabla_P^2}{8\pi^2 M}$$

$$+ V_{ne}(x, X) + V_{ee}(x) + V_{nn}(X)$$

x: coordinates of the electrons

X: coordinates of the nuclei

$M_A$ : mass of nucleus A

M: mass of the electron

$V_{ne}$ : electron-nuclear term:  $V_{ne}(x, X) =$

$$\sum_{iA} e^2 Z_A r_{iA}^{-1}$$

e: the charge of the electron

$Z_A$ : the charge on nucleus A

$V_{ee}$ : electron-electron repulsion term:

$$V_{ee}(x) = \sum_{p < q} e^2 r_{pq}^{-1}$$

$V_{nn}$ : the nuclear repulsion term

$$V_{nn}(X) = \sum_{A < B} Z_A Z_B e^2 / r_{AB}$$

If the wavefunction,  $\Psi$ , is constrained to be continuous, single valued, and to vanish at infinity, then there will be a number of solutions to the Schrodinger equation,  $\Psi_i$ , each with a discrete energy  $E_i$ . These eigenfunctions  $\Psi_i$  are called stationary, or bound, states of the system:  $H\Psi_i = E_i \Psi_i$ .

For a many particle system, it is clear that the solution of the Schrodinger Equation will be extremely difficult unless some simplifying approximations are made. The Born-Oppenheimer approximation states that, due to the rapid motion of electrons compared to nuclei the energy of the system can be reduced to the energy contribution of the nuclei and the electronic energy. The electronic Hamiltonian is described as:

$$H^{el} = \frac{-h^2}{8\pi m^2} \sum_p \nabla^2 - \sum_A \sum_p e^2 Z_A r_{pA}^{-1} + \sum_{p < q} e^2 r_{pq}^{-1}$$

Or, in atomic units

$$= \sum_p -\frac{1}{2} \nabla^2 - \sum_A Z_A \frac{1}{r_{pA}} + \sum_{p < q} \frac{1}{r_{pq}}$$

Thus,

$$H^{el}\psi = \epsilon\psi$$

and the total energy of a system for a fixed nuclear configuration is

$$E = \epsilon + \sum_{A < B} e^2 Z_A Z_B r_{AB}^{-1}$$

Since the concern of molecular orbital theory is the calculation of the electronic contribution, and evaluation of the nuclear term is straightforward, and is calculated separately, the superscript "el" will be dropped from the Hamiltonian for sake of convenience.

The electronic Hamiltonian can be further separated into terms  $H_1$  and  $H_2$ , the one and two electron operators:

$$\begin{aligned} H_1 &= \sum_p \left( -\frac{1}{2} \nabla^2 - \sum_A Z_A \frac{1}{r_{pA}} \right) \\ &= \sum_p H^c(p) \end{aligned}$$

$$H_2 = \sum_{p < q} 1/r_{pq}$$

Due to the indistinguishability of electrons the term  $H^C(1)$  will be identical to  $H^C(p)$ : thus

$$H_1 = NH^C(1)$$

N: the no. of electrons

similarly:

$$H_2 = \frac{1}{2}N(N-1)r_{12}^{-1}$$

The wavefunction,  $\Psi$ , can be approximated as a product of independent one electron functions,  $\Psi_i$ , which include a spin function, and will be referred to as spin orbitals. The product of spin orbitals must, as a result of the Pauli principle, be antisymmetrized:

$$\Psi(1,2,\dots,n) = \frac{1}{\sqrt{N!}} \{ \sum_i (-1)^{P_i} \Psi_1(1)\alpha(1)\Psi_1(2)\beta(2)\dots\Psi_n(2n)\beta(2n)\dots \}$$

$\alpha$ : the spin function such that:

$$S_Z^\alpha = \frac{1}{2} (h/2\pi)\alpha$$

$S_Z$  is the spin angular momentum operator for the Z component of the electron spin.

$\beta$ : the spin function such that:

$$S_Z^\beta = -\frac{1}{2}(h/2\pi)\beta$$

$P_i$ : a permutation operator which permutes the coordinates of the electrons. If the order, P, of  $P_i$  is odd, i.e., it permutes the coordinates of an odd number of electron pairs, the sign of that component of the wave function changes.

N: the no. of electrons

$\frac{1}{\sqrt{N!}}$ : normalization factor

The wavefunction,  $\Psi$ , is that of a closed shell state, that is, each space orbital is associated with two electrons, one with spin component  $S_z = +\frac{1}{2}$ , one with spin component  $S_z = -\frac{1}{2}$ . The rest of this section will concern closed shell states.

The determinantal expression for a closed shell state is:

$$\Psi(1,2,\dots,n) = \frac{1}{\sqrt{2n!}} \left| \begin{array}{c} \Psi_1(1) \bar{\Psi}_1(2) \dots \Psi_n(n-1) \bar{\Psi}_n(n) \end{array} \right|$$

$$\Psi_1(1) \equiv \Psi_1(1)\alpha(1)$$

$$\bar{\Psi}_1(2) \equiv \Psi_1(2)\beta(2)$$

Operating on  $\Psi$  with the Hamiltonian leads to the expression for the electronic energy of the system

$$\frac{\int \Psi^* H \Psi d\tau}{\int \Psi^* \Psi d\tau} = \epsilon = \int \Psi^* H \Psi d\tau: \text{ when orthonormal wavefunctions are used}$$

For a closed shell configuration, this is equivalent to

$$\epsilon = 2 \sum_i H_i + \sum_{ij} (2J_{ij} - K_{ij}) \quad \text{where } n = N/2$$

$$H_i: \int \Psi_i^* H^c(1) \Psi_i(1) d\tau_1$$

$$J_{ij}: \iint \Psi_i^*(1) \Psi_j^*(2) \frac{1}{r_{12}} \Psi_i(1) \Psi_j(2) d\tau_1 d\tau_2$$

$$K_{ij}: \iint \Psi_i^*(1) \Psi_j^*(2) \frac{1}{r_{12}} \Psi_i(2) \Psi_j(1) d\tau_1 d\tau_2$$

The term  $H_i$  is the contribution to the energy, of an electron in  $\Psi_i$  moving in the field of the bare nucleus, while  $J_{ij}$  is the interaction of the smoothed out charge distributions  $\Psi_i^* \Psi_i$  and  $\Psi_j^* \Psi_j$ , and is called the coulomb integral. The term  $K_{ij}$ , called the exchange integral, reduces the

interaction between electrons with like spin.

A set of one electron orbital energies can be described such that:

$$\epsilon_i = H_{ii} + \sum_j^n \{2J_{ij} - K_{ij}\}$$

where

$$\epsilon = 2 \sum_i^n \epsilon_i - \sum_{ij}^{nn} (2J_{ij} - K_{ij})$$

### The LCAO Approximation

To solve for the energy, the form of the one electron orbitals,  $\Psi_i$ , must be specified. The Linear Combinations of Atomic Orbital approximation, LCAO, defines the molecular orbital,  $\Psi_i$ , as the sum of atomic orbitals ( $\phi_\mu$ )

$$\Psi_i = \sum_\mu C_{\mu i} \phi_\mu$$

To meet the requirement of orthonormality:

$$\sum_{\mu\nu} C_{\mu i}^* C_{\nu j} S_{\mu\nu} = \delta_{ij}$$

where  $\delta_{ij}$  = Kronecker delta

and  $S_{\mu\nu} = \int \phi_\mu^*(1) \phi_\nu(1) d\tau$

The charge density can be defined:

$$\begin{aligned} \rho(R) &= \langle \Psi | \rho(R) | \Psi \rangle = 2 \sum_i^{\text{occ}} \Psi_i^*(R) \Psi_i(R) \\ &= \sum_{\mu\nu} P_{\mu\nu} \phi_\mu^*(R) \phi_\nu(R) \end{aligned}$$

where  $\langle \Psi | M | \Psi \rangle = \int \Psi^* M \Psi d\tau$

$$P_{\mu\nu} = 2 \sum_i^{\text{occ}} C_{\mu i}^* C_{\nu i}$$

and

$\rho(R)$  = charge density operator

Substitution of the LCAO molecular orbitals reduces the energy expression to:

$$\epsilon = \sum_{\mu\nu} P_{\mu\nu} H_{\mu\nu} + \frac{1}{2} \sum_{\mu\nu\lambda\sigma} P_{\mu\nu} P_{\lambda\sigma} [(\mu\nu|\lambda\sigma) - \frac{1}{2}(\mu\lambda|\nu\sigma)]$$

$$H_{\mu\nu} = \int \phi_{\mu}(1) H^C \phi_{\nu}(1) d\tau_1$$

$$J_{ij} = \sum_{\mu\lambda\nu\sigma} C_{\mu i}^* C_{\lambda j}^* C_{\mu i} C_{\nu j} (\mu\nu|\lambda\sigma)$$

$$K_{ij} = \sum_{\mu\lambda\nu\sigma} C_{\mu i}^* C_{\lambda j}^* C_{\nu i} C_{\sigma j} (\mu\lambda|\nu\sigma)$$

### The Roothaan Equations

The variation theorem, using the method of undetermined multipliers states that the best value of the energy of the system will be obtained by minimizing the function

$$G = \epsilon - 2 \sum_{ij} \epsilon_{ij} S_{ij}$$

$\epsilon_{ij}$  are the undetermined multipliers.

The minimum is found by finding a stationary point in the function such that  $\delta G = 0$  for a small change in the wavefunction  $\delta\Psi_i$ . In the LCAO approximation, the expression becomes:

$$\delta G = 2 \sum_i^{\text{occ}} \delta C_{\mu i}^* C_{\nu i} H_{\mu\nu} + \sum_{ij}^{\text{occ}} \sum_{\mu\nu\lambda\sigma} \{ (\delta C_{\mu i}^* C_{\lambda j}^* C_{\mu i} C_{\nu j} + C_{\mu i}^* \delta C_{\lambda j}^* C_{\nu i} C_{\sigma j})$$

$$[2(\mu\nu|\lambda\sigma) - (\mu\lambda|\nu\sigma)] \} 2 \sum_{ij\mu\nu} \epsilon_{ij} \delta C_{\mu i}^* C_{\nu j} S_{\mu\nu} + \text{complex conjugate} = 0$$

Since the  $\delta C_{\mu i}$  are arbitrary, the complete coefficient of each  $\delta C_{\mu i}^*$  must equate to zero. Thus, the equation leading to optimum values of  $C_{\mu i}$  is:

$$\sum_{\nu} \{ C_{\nu i} H_{\mu\nu} + \sum_j^{\text{occ}} \sum_{\lambda\sigma} C_{\lambda j}^* C_{\nu i} C_{\sigma j} [2(\mu\nu|\lambda\sigma) - (\mu\lambda|\nu\sigma)] \} = \sum_j \epsilon_{ij} \sum_{\nu} C_{\nu j} S_{\mu\nu}$$

It is possible, when convenient, to demand that

$\epsilon_{ij} = 0$  unless  $i = j$ , without loss of generality. Thus, the equation reduces to:

$$\sum_{\nu} (F_{\mu\nu} - \epsilon_i S_{\mu\nu}) C_{\nu i} = 0$$

$$F_{\mu\nu} = H_{\mu\nu} + \sum_{\lambda\sigma} P_{\lambda\sigma} \{ (\mu\nu|\lambda\sigma) - \frac{1}{2}(\mu\lambda|\nu\sigma) \}$$

These equations, known as the Roothaan equations, must be solved iteratively. They can be written, in matrix notation, as

$$FC = SCE$$

### Unrestricted Molecular Orbitals

When an excited state of a molecule is formed, an electron is considered as being removed from an occupied orbital of the ground state to an unoccupied orbital. If we are considering one in which the number of alpha electrons differs from the number of beta electrons, say a triplet state, the wavefunction will be written:

$${}^3\Psi = |\psi_1(1)\bar{\psi}_1(2)\dots\bar{\psi}_q(2q)\psi_{q+1}(2q+1)\dots\psi_p(p+q)|$$

$p$ : the no. of alpha electrons

$q$ : the no. of beta electrons

However, as there is an excess of alpha spin, then the environment of alpha electrons will differ from that of beta electrons. Thus, the spatial wavefunctions,  $\psi_1$ , say, is allowed to differ for alpha and beta electrons. Therefore,  $\psi_1(1)$  becomes  $\psi_1^\alpha(1)$  and  $\bar{\psi}_1(2)$  becomes  $\bar{\psi}_1^\beta(2)$  and is calculated separately from  $\psi_1$ . Thus the new wavefunction becomes:

$${}^3\Psi = |\psi_1^\alpha(1)\bar{\psi}_1^\beta(2)\dots\bar{\psi}_q^\beta(2q)\psi_{q+1}^\alpha(2q+1)\dots\psi_p^\alpha(p+q)|$$



and is the unrestricted wavefunction. It can be shown that Roothaan's equations for an unrestricted wavefunction will become:

$$F_{\mu\nu}^{\alpha} = H_{\mu\nu} + \sum_{\lambda\sigma} [P_{\lambda\sigma}(\mu\nu|\lambda\sigma) - P_{\lambda\sigma}^{\alpha}(\mu\sigma|\lambda\nu)]$$

$$F_{\mu\nu}^{\beta} = H_{\mu\nu} + \sum_{\lambda\sigma} [P_{\lambda\sigma}(\mu\nu|\lambda\sigma) - P_{\lambda\sigma}^{\beta}(\mu\sigma|\lambda\nu)]$$

$$\sum_{\nu} (F_{\mu\nu}^{\alpha} - \epsilon_i^{\alpha} S_{\mu\nu}) C_{\nu i}^{\alpha} = 0$$

$$\sum_{\nu} (F_{\mu\nu}^{\beta} - \epsilon_i^{\beta} S_{\mu\nu}) C_{\nu i}^{\beta} = 0$$

These equations are varied independently and:

$$\epsilon = \sum_{\mu\nu} P_{\mu\nu} H_{\mu\nu} + \frac{1}{2} \sum_{\mu\nu\lambda\sigma} (P_{\mu\nu} P_{\lambda\sigma} - P_{\mu\lambda}^{\alpha} P_{\nu\sigma}^{\alpha} - P_{\mu\lambda}^{\beta} P_{\nu\sigma}^{\beta}) (\mu\nu|\lambda\sigma)$$

### The Complete Neglect of Differential Overlap (CNDO) Method<sup>5,6,7</sup>

The CNDO method, first introduced by Pople, Santry, and Segal<sup>6,7</sup> is a semi-empirical method which makes use of the zero differential overlap approximation. The CNDO method treats only the valence electrons and assumes the inner electrons, the so-called core electrons, do not significantly effect the bonding. These core electrons are treated as point charges on the nucleus, thus reducing the effective nuclear charge.

In the CNDO approximation, many of the one electron integrals are replaced by constants which are derived from experiments.

### The Zero Overlap Approximation.

The zero overlap approximation states that any electron repulsion integral involving an overlap distribution can be neglected:

$$(\mu\nu|\lambda\sigma) = (\mu\mu|\lambda\lambda) \delta_{\mu\nu} \delta_{\lambda\sigma}$$

and also neglects the overlap integral in the normalization of molecular orbitals. The core integrals,  $H_{\mu\nu}$ , involving overlap integrals are, however, not neglected but are treated semi-empirically. The integrals are included to accommodate the bonding effect of overlap.

The core integrals are divided into diagonal and off-diagonal elements:

$$\begin{aligned}
 H_{\mu\mu} &= U_{\mu\mu} - \sum_{B \neq A} (\mu | V_B | \mu) \\
 H_{\mu\nu} &= U_{\mu\nu} - \sum_{B \neq A} (\mu | V_B | \nu) && \phi_\mu, \phi_\nu \text{ on A} \\
 U_{\mu\mu} &= (\mu | -1/2\nabla^2 - V_A | \mu) \\
 H_{\mu\nu} &= (\mu | -1/2\nabla^2 - V_A - V_B | \nu) - \sum_{C (\neq A, B)} (\mu | V_C | \nu) && \begin{array}{l} \phi_\mu \text{ on A} \\ \phi_\nu \text{ on B} \end{array}
 \end{aligned}$$

For the  $H_{\mu\nu}$  term where  $\mu \neq \nu$ , both on centre A,

the term  $U_{\mu\nu}$  vanishes by orthogonality, provided the orbitals are of the type S, P, etc. and not hybrids. The zero overlap approximation neglects all monatomic overlap, thus, the term  $(\mu | V_B | \nu)$  will vanish. The terms  $(\mu | V_B | \mu)$  are taken to be independent of the nature of the orbitals  $\phi_\mu$ . Thus, the term  $(\mu | V_B | \mu)$  is replaced by  $V_{AB}$ .

The integrals  $(\mu | V_C | \nu)$  are neglected, as before, and the remaining term  $H_{\mu\nu}$  for  $\mu$  on A,  $\nu$  on B is replaced by  $\beta_{\mu\nu}$ , the resonance integral. In this case, the overlap integral is not neglected. This will account for possible bonding effects of overlap, and the term  $\beta_{\mu\nu}$  is treated semi-empirically. This is accomplished by replacing  $\beta_{\mu\nu}$  as:

$$\beta_{\mu\nu} = \beta_{AB}^0 S_{\mu\nu}$$

where

$$\beta_{AB}^0 = \frac{1}{2}(\beta_B^0 + \beta_A^0)$$

The term  $\beta_A^0$  depends only on the nature of the atom, A, and is obtained by comparing, over a range of molecules, CNDO calculations with good "ab initio" calculations. The values are obtained by a best fit technique.

The Roothaan Equations, upon substitution of the zero differential overlap approximation, become

$$\sum_{\nu} F_{\mu\nu} C_{\nu i} = \epsilon_i C_{\mu i}$$

or, in matrix notation,

$$FC = CE$$

The elements of the Fock matrix, R, are defined as:

$$F_{\mu\mu} = H_{\mu\mu} - \left(\frac{1}{2}\right) P_{\mu\mu} (\mu\mu|\mu\mu) + \sum_{\lambda} P_{\lambda\lambda} (\mu\mu|\lambda\lambda)$$

$$F_{\mu\nu} = H_{\mu\nu} - \left(\frac{1}{2}\right) P_{\mu\nu} (\mu\mu|\nu\nu)$$

### The Parameterization<sup>9,10</sup>

Having substituted values for the term  $\beta_{\mu\nu}$  there remain other integrals to be evaluated. As a result of the zero differential overlap approximation all two electron terms are of the form:

$$\begin{aligned} (\mu\nu|\lambda\sigma) &= (\mu\mu|\lambda\lambda) \delta_{\mu\nu} \delta_{\lambda\sigma} \\ &= \gamma_{AB} \end{aligned}$$

$\gamma_{AB}$  is, then, the average repulsion felt by any electron on centre A due to the field of any electron on centre B. This term is independent of the nature of the atomic orbital  $\phi_{\mu}$ , and depends only on the nature of the two atoms. In CNDO/2, these integrals are evaluated in a straightforward manner, using the S valence orbitals as the functions:

$$\gamma_{AB} = \iint S_A^2(1) (r_{12})^{-1} S_B^2(2) d\tau_1 d\tau_2$$

The core matrix,  $H_{\mu\mu}$ , is expressed as above:

$$H_{\mu\mu} = U_{\mu\mu} - \sum_{B(\neq A)} V_{AB} \quad \phi_{\mu} \text{ on A}$$

$$H_{\mu\nu} = 0 \quad \phi_{\mu} \neq \phi_{\nu}$$

both on A

$$H_{\mu\nu} = S_{\mu\nu} \beta_{AB}^0 \quad \phi_{\mu} \text{ on A}$$

$\phi_{\nu}$  on B

The overlap matrix is evaluated in a straightforward manner. The term  $V_{AB}$  is evaluated in a similar manner to  $\gamma_{AB}$ , in that, the term is independent of the orbital,  $\phi_{\mu}$ , and the S valence orbitals are used as functions. As the term is the interaction between any electron on A with the core plus nucleus on B,  $V_{AB}$  is:

$$V_{AB} = Z_B \int S_A^2(1) (r_{1B})^{-1} d\tau_1$$

$Z_B$  = the effective nuclear charge on B.

The term  $U_{\mu\mu}$  is defined as follows:

$$U_{\mu\mu} = -\frac{1}{2} (I_{\mu} + A_{\mu}) - (Z_A - \frac{1}{2}) \gamma_{AA}$$

$I_{\mu}$  = the ionization potential from orbital  $\phi_{\mu}$  centred on Atom A.

$A_{\mu}$  = the electron affinity of orbital  $\phi_{\mu}$  on centre A

Substitution of the newly parametrized terms into the

Fock matrix results in:

$$F_{\mu\mu} = U_{\mu\mu} + (P_{AA} - \frac{1}{2} P_{\mu\mu}) \gamma_{AA} + \sum_{B(\neq A)} (P_{BB} \gamma_{AB} - V_{AB})$$

$$F_{\mu\nu} = \beta_{AB}^0 S_{\mu\nu} - (\frac{1}{2}) P_{\mu\nu} \gamma_{AB} \quad \mu \neq \nu$$

$$P_{AA} = \sum_{\lambda} A_{P_{\lambda\lambda}}$$

The term  $(P_{BB} \gamma_{AB} - V_{AB})$  can be factored:

$$(P_{BB} \gamma_{AB} - V_{AB}) = -Q_B \gamma_{AB} + (Z_B \gamma_{AB} - V_{AB})$$

$$Q_B = Z_B - P_{BB}$$

The quantity  $(Z_B \gamma_{AB} - V_{AB})$  is the difference in potential between the valence electrons and the core of the central atom, and is termed the penetration integral. This term is neglected in CNDO/2, as it is responsible for calculated bonding energies between centers where there is no bond order<sup>3</sup>. Thus, the term  $V_{AB}$  is replaced:

$$V_{AB} = Z_B \gamma_{AB}$$

and the element of the Fock Matrix becomes:

$$F_{\mu\mu} = U_{\mu\mu} + (P_{AA} - (\frac{1}{2}) P_{\mu\mu}) \gamma_{AA} + \sum_{B(\neq A)} (P_{BB} \gamma_{AB} - V_{AB})$$

and

$$F_{\mu\nu} = \beta_{AB}^0 S_{\mu\nu} - (\frac{1}{2}) P_{\mu\nu} \gamma_{AB} \quad \mu \neq \nu$$

in which each of the terms has been evaluated. The expression for the energy becomes:

$$\epsilon_{\text{total}} = (\frac{1}{2}) \sum_{\mu\nu} P_{\mu\nu} (H_{\mu\nu} + F_{\mu\nu}) + \sum_{A < B} Z_A Z_B r_{AB}^{-1}$$

where  $\sum_{A < B} Z_A Z_B r_{AB}^{-1}$  is the nuclear repulsion term.

The Solution of Roothaans Equations 3-7, 12, 13

To solve the Roothaan's equations, an iterative procedure is followed.

The value of the overlap matrix,  $S_{\mu\nu}$ , is determined and then the Fock matrix is replaced by the following approximation:

$$F_{\mu\mu} = \beta_{AB}^0 S_{\mu\gamma}$$

$$F_{\mu\mu} = U_{\mu\mu}$$

The approximate Fock matrix is then diagonalized and the electrons are assigned in pairs (for a closed shell state) to the appropriate molecular orbitals (the lowest set for a ground state, etc). The density matrix,  $P$ , is evaluated from the coefficient matrix,  $C$ , formed in the diagonalization of  $F$  approx.:

$$P_{\mu\gamma} = \sum_i^{occ} C_{\mu i} C_{\gamma i}$$

The sum being over all occupied orbitals.

Thus, having  $P_{\mu\nu}$ , a new Fock matrix can be constructed,  $F$ , and the procedure is carried out until self-consistency is obtained. The degree of self-consistency is usually monitored by the convergence of the energy, the expression for which is given above. Thus, the pattern of the iterative method is, after evaluation of integrals:

$$\begin{array}{cccccccc} F & \rightarrow & C & \rightarrow & P & \rightarrow & F & \rightarrow & C & \rightarrow & P & \rightarrow & F & \text{etc} \\ \downarrow \text{app} & & & & & & \downarrow & & & & & & \downarrow & \\ E & & & & & & E & & & & & & E & \end{array}$$

Configuration Interaction<sup>3-6</sup>

In Hartree-Fock theory, the wavefunctions of a many

electron system are constructed as the product of linearly independent one electron wavefunctions. The wavefunction of a molecule is, then, the product of so-called molecular orbitals. The molecular orbitals describe the motions of electrons about the nucleus and, when multiplied by the spin function of the electrons "occupying" these orbitals, are the one electron wavefunctions above. By virtue of the nature of the approximation, the motions of electrons in molecular orbital theory are independent of the other electrons. Thus, the probability of two electrons being in a particular region of space is merely the product of the probabilities of each electron being in that region, independent of the presence of the other. This clearly will be too high, resulting in an overestimation of electron repulsion terms, and an underestimation of the calculated binding energy<sup>3-6</sup>.

The contribution to the calculated energy of the system by the lack of correlated electronic motion, is called the correlation energy. The most accurate Hartree-Fock calculation must be in error by, at least this amount, thus, defining the Hartree-Fock limit:

$$E_{\text{HF}} = E_{\text{ex}} - E_{\text{co}}$$

$E_{\text{HF}}$ : the Hartree-Fock energy

$E_{\text{ex}}$ : the true energy

$E_{\text{co}}$ : the correlation energy

The correlation energy is often quite large, usually of the same order as the binding energy.

It has been shown<sup>3-6</sup> that, as well as giving rise to a poor estimate of binding energies, Hartree-Fock wavefunctions give poor correlation of electronic states of a molecule with dissociation products. To correct this, the method of Configuration Interaction (CI) is used<sup>1-4</sup>. The CI wavefunction of a state  $\Psi_i^c$  is expressed as the sum of a set of Hartree-Fock wavefunctions,  $\Psi_j$ , multiplied by a mixing coefficient,  $C_{ij}$ , thus:

$$\Psi_i^c = \sum_j C_{ij} \Psi_j$$

The variation theorem is used to optimize these coefficients.

In the calculations observed below, the set of interacting states was constructed from the virtual orbitals of the ground state, and the elements of the CI matrix were calculated in a straightforward manner<sup>1-4,11</sup>. A list of non-zero off diagonal elements is tabulated below (see Table I). The diagonal elements of the interaction matrix are merely the energy of the Hartree-Fock states  $\Psi_i$ .

The number of states used in the CI calculation was limited to all single excitation states and all states observed by placing two electrons in a virtual orbital at the expense of both electrons from one occupied orbital. All other states were excluded as the effect of interest in the correlation of states with product rather than the exact energy of a state. That this exclusion of other states will not seriously effect the calculation can be seen from second order perturbation theory: the second order correction to the energy,  $E_2$ , of a state,  $\Psi_i$  is:

$$E_2 = \sum_j E_j^{(2)}$$

$$E_j^{(2)} = A_{ij}^2 / E_i - E_j$$

$$A_{ij} = \langle \Psi_i | H | \Psi_j \rangle$$



When the difference in energy  $E_i - E_j$ , is large,  $E_j^{(2)}$  will be small. As the states excluded will be of high energy, then the arbitrary exclusion of these states will not adversely affect the calculation to too great an extent.

TABLE 1

The Matrix Elements of the Interaction Matrix: off diagonal elements \* \*\*

<u>Interaction states:</u>		<u>Matrix element:</u>
<u>State 1</u>	<u>State 2</u>	
i → k	j → n	$2[(jn   ik) - (ji   nk)]$
i → k	i → n	$H_{kl} + \sum^m 2[(jj   kn) - (jn   kj) + 2(in   ki) - (ii   kn)]$ M: any orbital occurring in both states.
i → k	j → k	$-[H_{ji} + \sum_{n=1}^m (2(nn   ji) - (ni   jn))] + 2(ki   jk) - (kk   ji)$
ii → nn	jj → nn	$(ji   ji)$
i → k	jj → kk	$-\sqrt{2} (ji   ji)$
i → n	ii → kk	$\sqrt{2} (ik   nk)$
i → k	ii → kk	$\sqrt{2} (kk   ik) - (ii   ki)$
0	ii → kk	$(ik   ki)$
ii → nn	ii → kk	$(nk   nk)$

\* These are states of symmetry  ${}^1A_1$ , all other states will have vanishing matrix elements.

\*\* The symbols denote the molecular orbitals involved in the promotion of an electron, or acceptance of an electron. All other mo are the same in both states.

Chapter II

Review of Experimental Information

The Spectroscopy Carbonyl Compounds

Carbonyl compounds show a number of spectroscopic transitions in the ultraviolet region. The lowest lying transition has been assigned as the  $(\pi^* \leftarrow n)^{14-17}$  transition, that is, an excitation of an electron from a non-bonding orbital (which is usually considered as the 2P lone pair orbital centred on the oxygen) to an antibonding  $\pi$  orbital centred between the carbon and oxygen atoms. This transition is normally around 3.6 eV (340 nm) and has a low extinction coefficient,  $\epsilon \cong 15^{14-17}$ .

There is a transition at about 6.5 eV (140 nm) with  $\epsilon = 1400^{14,18,19}$ . There has been disagreement in the literature as to its assignment. The transition has been assigned as  $\pi^* \leftarrow n^{14,18}$  while other researchers have proposed  $\sigma_{CO}^* \leftarrow n^{20,21}$ . A third transition, considered to be a Rydberg transition<sup>14,18</sup> is observed for many carbonyl compounds in the region of 8.3 eV (150 to 160 nm). The intense transition,  $\epsilon \cong 4000$ , which occurs at about 9 eV<sup>19,20</sup>, has been assigned to the  $\pi^* \leftarrow \pi$  transition.

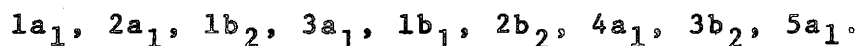
The observed transitions in the formaldehyde system are<sup>14,18</sup>:

360 to 390 nm	<sup>3</sup> ( $\pi^* \leftarrow n$ )
350 to 280 nm	<sup>1</sup> ( $\pi^* \leftarrow n$ )

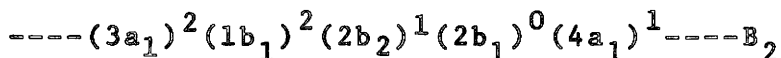
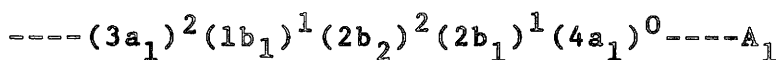
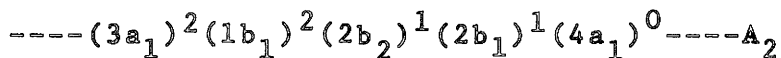
There is a transition at 175 to 165 nm which has been assigned by some researchers<sup>21</sup> as a ( $\sigma^* \leftarrow n$ ) , or ( $\pi^* \leftarrow n'$ ) transition, but it has been established as the first of a series of four Rydberg states, starting at 175.6, 155.6, 152.4 and 139.7 nm<sup>15,18</sup>. No assignment has been made of the ( $\pi^* \leftarrow \pi$ ) state which probably lies in the region beyond the Rydberg states, a region which has not received much attention.

### The molecular orbitals of Formaldehyde

Formaldehyde in the ground state, is a planar molecule of the  $C_{2v}$  point group. There are a total of 16 electrons in all, of which we will consider only 12. The 1s electrons of both the carbon and oxygen atoms do not contribute very much to the high energy molecular orbitals (mo) of formaldehyde, and, as these are the mo's responsible for the photochemistry, the inner electrons can be, to a reasonable approximation, ignored. The 10 atomic orbitals (ao's), occupied by these electrons, give rise to 10 mo's, the symmetry labels of which are listed in order of increasing orbital energies:



The 12 electrons will doubly occupy the lowest 6 orbitals, giving rise to a  $^1A_1$  ground state. The excited state configuration will arise by populating the one or more of the vacant orbitals at the expense of the occupied orbitals. Each configuration will give rise to a number of states. Some of the low lying excited states are constructed below.



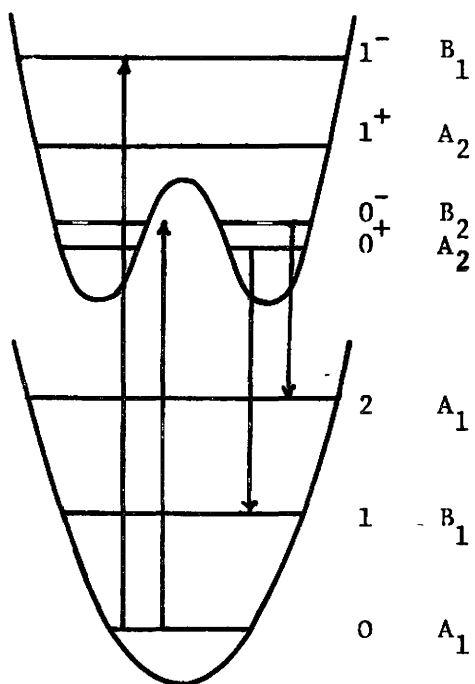
The superscripts indicate the number of electrons in the mo. As the excitations involve only one electron, these configurations will give rise to two states each, a singlet and a triplet.

The molecular orbitals are, for convenience, often described by terms carried over from the nomenclature of diatomic species. Thus, in the case of formaldehyde, we will have two types of bonds,  $\sigma$  bonds and  $\pi$  bonds. The  $\sigma$  bond is directed along the internuclear axes, and extends, in general, over the whole molecule. The  $\pi$  bond, assuming the molecule remains planar, is a result of overlap between the  $2p_z$  orbitals of carbon and oxygen. As a result of orthogonality, it receives contributions from no other atomic orbitals. Thus it lies above and below the molecular plane, and is concentrated in the region between the carbon and oxygen atoms. If, however, the molecule deviates from planarity, a contribution will result from the hydrogen atoms, and the orbital will cease to be a pure  $\pi$  orbital.

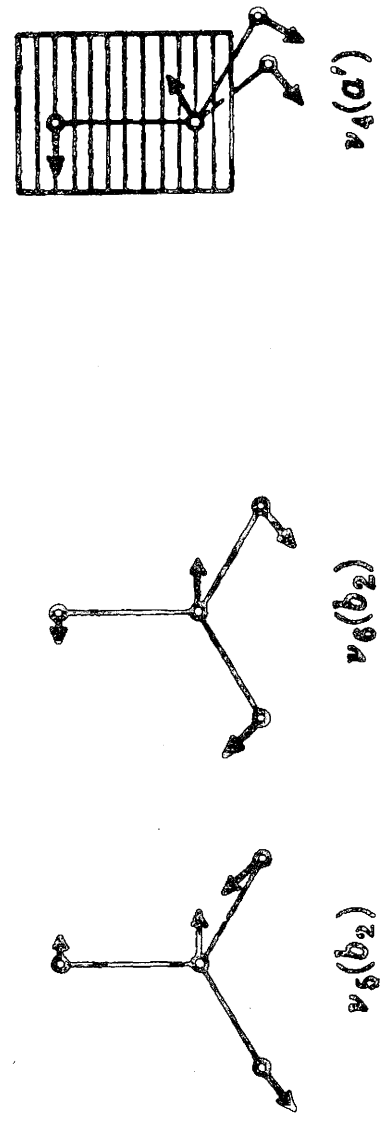
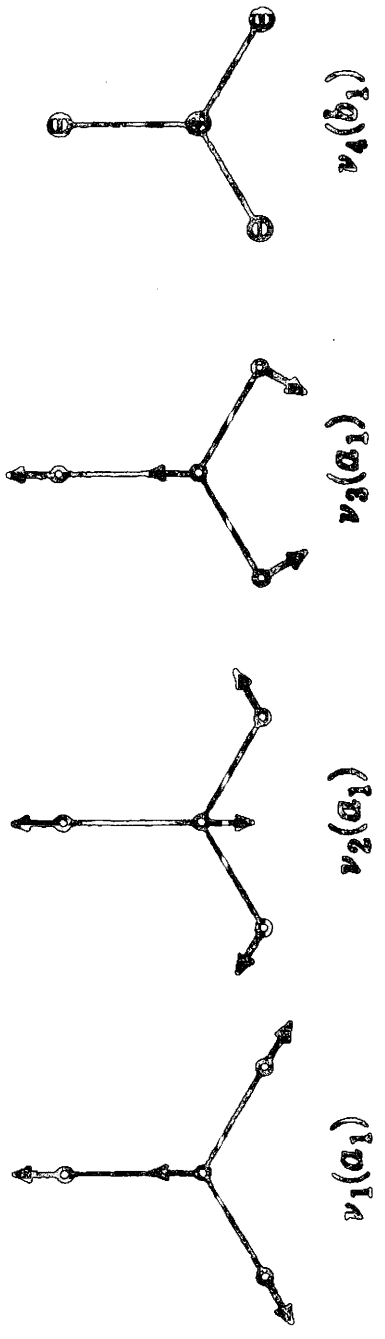
The orbitals can be classified further with respect to their contribution to the bonding or antibonding character of the molecule, i.e., whether they will raise or lower the total energy of the molecule with respect to separate  $\alpha$  atoms. This arises from either positive or negative overlap between the various atomic

orbitals. The  $\pi$  orbitals, as they involve only two centres, are either bonding or antibonding. The  $\sigma$  orbitals, as they involve more than two centres can have positive overlap between some ao's while negative with others, the bonding then being the net effect. Thus a orbital may be bonding overall, or bonding between some centres and antibonding between others. There is a special case where the total bonding effect of an orbital is negligible, these orbitals being designated n. The  $2b_2$  orbital, although slightly bonding is so designated. Thus the state  $^1A_2$ , which arises out of the configuration  $---(2b_2)^1(2b_1)^1, ^1, ^3A_2$ , is designated  $^1, ^3n, \pi^*$ , similarly the  $^1, ^3A_1$  is  $^1, ^3\pi, \pi^*$ , and the  $^1, ^3B_2$  is  $^1, ^3n, \sigma^*$ . The asterisk superscript designates overall antibonding. The  $\sigma^*$  orbitals are often given a subscript to denote the centres between which they are antibonding; thus  $\sigma_{CO}^*$  and  $\sigma_{CH_2}^*$  indicates they are anti-bonding between the carbon and oxygen atoms and the carbon and hydrogen atoms respectively.

The low lying excited state in  $H_2CO$  has been assigned to the  $^1(\pi^* \leftarrow n)$  transition and has been well characterized<sup>14,15,18</sup>. The absorption extends over the range 320 nm to 220 nm and contains considerable fine structure, with a continuum setting in at the short wavelength region. The singlet triplet absorption, i.e.,  $^3A_2 \leftarrow ^1A_1$  is also observed from 365 to 393.7 nm and also contains considerable fine structure<sup>14,15,18</sup>. This  $(\pi^* \leftarrow n)$  transition is electronically forbidden but, due to coupling

Figure I: The Allowed Transitions of Formaldehyde in the  $C_{2v}$  Point Group

The transitions are:  $A_1 \longleftrightarrow B_2$ ;  $B_1 \longleftrightarrow A_2$



The Normal Vibrational Modes of Formaldehyde



of the electronic function with the  $\nu_4^{14,15,18,19}$  out of plane bending vibration, (see fig. II) the transition is vibronically allowed. The upper electronic state,  $^1A_2$ , has been shown to be non-planar,  $^{14,15,18,19}$  and is, therefore, a member of the  $C_s$  point group and should be classified  $^1A''$ . The barrier to inversion is very small,  $650 \text{ cm}^{-1}$ , and results in inversion doubling in the levels of the  $\nu_4$  vibration  $^{14,15,18,19}$ .

The selection rule for the transition can be determined by describing the transition either in terms of a  $^1A' \leftarrow ^1A''$  or  $^1A_1 \leftarrow ^1A_2$  transition. For convenience they will be determined in the  $C_{2v}$  point group. For the transition moment to be non-zero the integral

$$\langle \Psi' | r | \Psi \rangle$$

$\Psi$ : is the wavefunction of the lower state;

$\Psi'$ : is the wavefunction of the upper state;

$r$ : the transition dipole moment operator.

must transform as  $A_1$ . The electronic wave function of the ground state is  $A_1$ , that of the upper state is  $A_2$ . The operator has three components:

x axis:  $b_2$

y axis:  $a_1$

Z axis:  $b_1$

The vibrational wave-functions in the ground state transform for even levels as  $A_1$ , and for odd levels as  $B_1$  (see fig. 1). The upper state, as it is inversion doubled, has the levels  $0^+ 0^-$ ,  $1^+ 1^-$ , etc. The plus levels of the vibrational

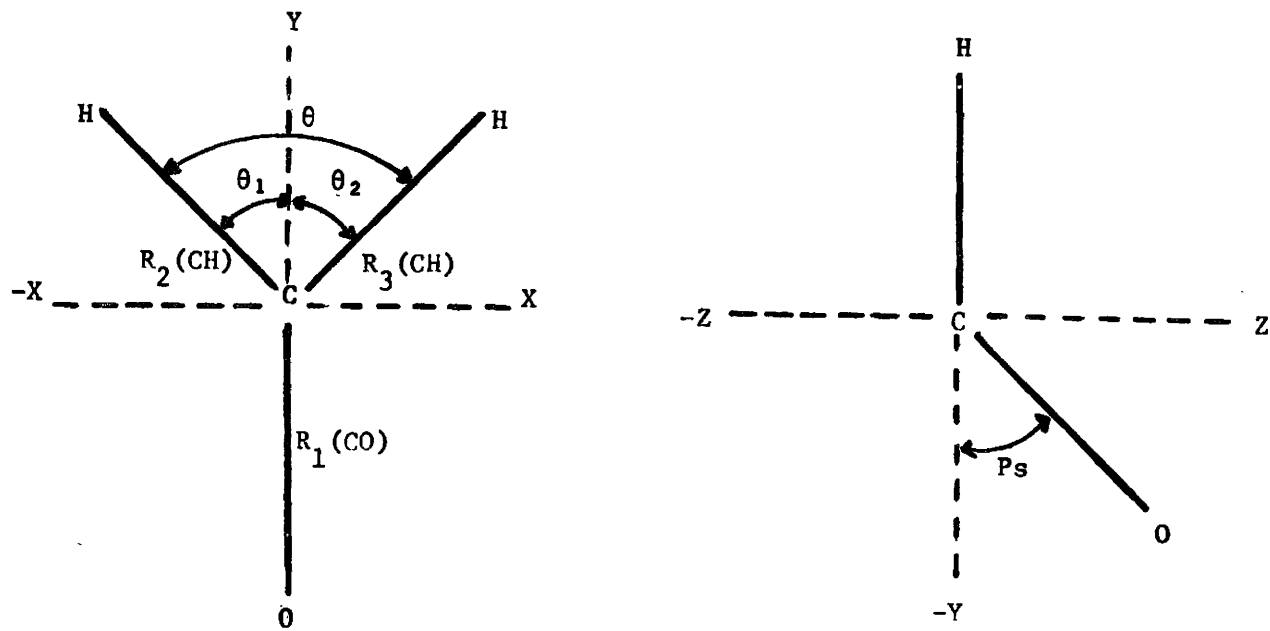


Figure III: The Coordinate System of Formaldehyde

wavefunctions transform as  $A_1$ , the minus levels as  $B_1$ . Thus the vibronic wavefunctions of the ground state transforms alternately as  $A_1$  and  $B_1$ , while that of the upper state as  $A_2$  and  $B_2$ . Thus transitions between the  $A_1$  and  $B_2$ , and  $B_1$  and  $A_2$  levels are allowed with the  $B_2$  components of the transition moment operation, and are called perpendicular transitions.

In the absorption spectra there are a series of parallel bands which are transitions between even-even and odd-odd levels of the ground and upper states which are very weak and have been identified as magnetic dipole induced transitions<sup>19,20</sup>.

The lifetime of the  ${}^1n,\pi^*$  state of  $H_2CO$  has been measured recently from emission in the gas phase<sup>22</sup>. The level excited was that involving the  $1^-$  level of  $\nu_4$  and 1 quanta of  $\nu_6$ . The lifetime was 27 nsecs. and is independent of pressure in the region 0.3 to 3.8 torr; the emission observed was from 420 to 500 nmeters. Unfortunately, the level excited does not emit, so that the lifetime observed will be that of the  $0^{\pm}$  levels of the singlet, provided equilibration to this level is fast compared to the lifetime of the emitting state.

The lifetime of the  $D_2CO$   ${}^1n,\pi^*$  state has also been reported<sup>23</sup>. For excitation of 3 quanta of  $\nu_2'$  (C = O stretch) the lifetime is found to be 103 nsecs, independent of pressure in the region 0.1 to 10 torr. However, excitation to the  $1^-$  level of  $\nu_4'$  gives a pressure

dependent lifetime, varying from 5 nsecs at 0 torr to 66 nsecs at 10 torr. However, as in the previous case, the emitting state is not the one excited, but the  $0^-$  level of  $\psi_4'$ .

An estimate of the lifetime of the  $1^\pm$  levels of  $\psi_4'$  in  $H_2CO$  can be made. As there is no evidence of predissociation in the absorption spectra to this level, then natural line width,  $\Delta W$ , cannot exceed  $0.1 \text{ cm}^{-1}$ , the Doppler broadening for the temperature at which these spectra are taken. The line width is given by the following relationship<sup>24</sup>:

$$\Delta W = \frac{1}{2\pi c} \left( \frac{1}{\tau_o} + \frac{1}{\tau_t} \right)$$

$c$  = speed of light

$\tau_o$  = natural radiative lifetime

$\tau_t$  = the mean lifetime of the  
non-radiative processes.

for  $W$  to exceed  $0.1 \text{ cm}$ , the total  $\left( \frac{1}{\tau_o} + \frac{1}{\tau_t} \right)$  must exceed a value of  $10^{10}$ . Since the natural radiative lifetime, is of the order of  $10^{-5} \text{ sec}$ <sup>25</sup>, then  $\tau_t$  must be no greater than  $10^{-10}$ . The quantum yield of emission,  $\phi_e$ , is defined as the amount of light emitted by a particular level, divided by the light absorbed in exciting that level; thus, an undetectable emission will correspond, for a molecule with a low extinction coefficient such as  $H_2CO$ , to a quantum yield of emission of no greater than 0.001. Defining the

quantum yield as  $\tau_0 + \tau_t/\tau_0 \cong \tau_t/\tau_0$ , then  $\tau_t/\tau_0 \cong 0.001$ . Thus,  $\tau_t$  is at least  $10^{-8}$ , and the rate constant for non-radiative process depopulating the  $1\pm$  levels of  $\gamma_4'$  in the  $1_n, \pi^*$  state of formaldehyde lies in the region  $10^8$  to  $10^{10} \text{ s}^{-1}$ .

The emission spectra, in the gas phase of the  $1_n, \pi^*$  state are independent of the excitation source, that is, the fluorescence and discharge spectra are identical<sup>14,15</sup>. There has been no evidence reported of triplet involvement in the vapour phase emission spectra<sup>15,20</sup>. The only levels from which emission is observed in the  $1_n, \pi^*$  state of  $\text{H}_2\text{CO}$  are the  $0^\pm$  levels of  $\nu_4'$  and the first level of  $\nu_2'$ . A very weak emission is also observed from the level in which two quanta of  $\nu_2'$  are excited. The  $\text{D}_2\text{CO}$  spectra is similar, with the exception that the  $1^\pm$  levels of  $\nu_4'$  are also active in emission<sup>14,15</sup>.

### The Photochemistry of $\text{H}_2\text{CO}$

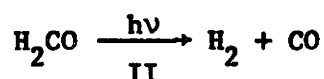
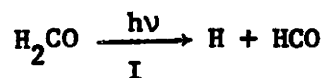
The spectroscopic analysis of the formaldehyde<sup>14,15</sup>  $1,3_n, \pi^*$  states, despite the detailed studies, has yielded little information on the nature of the photon induced processes that lead to decomposition. The considerable fine structure in the absorption and emission spectra indicates a stable upper state. The vanishingly small intensity from the  $1^\pm$  levels of the  $\nu_4'$  vibrational mode, in the emission from the upper state, puts a lower limit of predissociation of about 82 kcal/mole<sup>14,15</sup>. The lack of emission from these levels, although the absorption of

these levels is well resolved, indicates that the rate constants of the non-radiative processes depopulating this level are of the order of from  $10^8 \text{ sec}^{-1}$  to  $10^{10} \text{ sec}^{-1}$ .

Evidence for triplet involvement in the photochemistry comes from two sources. Degraff and Calvert<sup>16</sup>, on the basis of a study in which mixtures of biacetyl and formaldehyde- $d_2$  were irradiated at 3130 Å, found phosphorescence of biacetyl preferentially excited. In a study conducted by Smith and Meyer<sup>17</sup> of matrix isolated formaldehyde at low temperature, phosphorescence emission was observed. The lifetime of this emission was measured as  $1.1 \pm 0.2$  secs. at 20°K in Krypton. The lifetime was dependent upon the temperature and the matrix material but the radiative lifetime of the triplet of formaldehyde can be given a lower limit of 1.1 secs. Thus, this places an upper limit on  $k_p$ , the rate constant of phosphorescence emission, as approximately  $0.9 \text{ sec}^{-1}$ . Thus, the triplet can have a role in the decomposition processes and yet not be observed in the gas phase by emission, as the rate constant for emission is so low.

Further information about the formaldehyde photochemical system comes from studies of the decomposition yields<sup>16,26,27</sup>. This study is, however, complicated by virtue of a tendency of formaldehyde to polymerize at room temperature, while a chain reaction is initiated at temperatures high enough to prevent this polymerization. The chain is sufficiently large at temperature of 300°C

that excitation at 313 nm has a  $\phi_d$  of the order of 100, while it drops to a value near unity at 100°C<sup>5</sup>, where  $\phi_A$  is defined as: (no. of molecules undergoing process A)/(no. of molecules absorbing light). Thus, extensive temperature studies are not feasible. The decomposition results mainly in the products H<sub>2</sub> and CO<sup>26-28</sup>, with decomposition being postulated to occur via two mechanisms:



There is conflicting evidence in the literature concerning the wavelength dependence of these two processes. Iodine inhibition studies and isotope scrambling studies<sup>26,27,29</sup> indicate that, at temperatures near 100°, the ratio  $\phi_{\text{II}}/\phi_{\text{I}}$  is proportional to wavelength, that is  $\phi_{\text{II}}$  predominates over  $\phi_{\text{I}}$  at larger wavelengths. The radical trapping study of Degraff and Calvert<sup>16</sup>, however, shows an opposite effect. That study has been criticized<sup>29</sup> because the amount of inhibitor required to remove all radicals was only calibrated for one wavelength, 313 nm. As a result, any radical produced H<sub>2</sub> arising due to insufficient trapping would be attributed to process II instead of process I.

Klein and Schoen<sup>27</sup> observed the ratio of  $\phi_{\text{II}}/\phi_{\text{I}}$  as a function of pressure at 3655 Å. It was found to be 2.0 at a pressure of 26.8 torr while at a pressure of 221.9 torr, the ratio was 0.2. This study was carried out at 140°C, where the chain length is near unity, and the excitation is to the lowest vibrational levels of the upper state. As a result,

the only effect of pressure would be thermal excitation to higher levels of the upper state. This would explain the anomalously low predissociation limit for formaldehyde, = 82 kcal/mole as opposed to  $D_{\text{H-COR}}$  of 85 kcal/mole for such molecules as acetaldehyde<sup>29</sup>. Photoionization experiments lead to a value of  $85.1 \pm 1.4$  kcal/mole<sup>30</sup> for D-CHO, while Walsh and Bension<sup>31</sup> find a value of  $87 \pm 0.1$  kcal/mole from kinetic studies. Thus, if the formaldehyde, upon being excited with 365 nm radiation, can be thermally excited to the higher vibrational levels, then the observation of radical products<sup>26,27,29</sup> from excitation at this wavelength is consistent with a dissociation limit higher than the energy absorbed.

While the evidence is quite strongly in agreement with an increase in the ratio of  $\phi_{\text{II}}/\phi_{\text{I}}$  with increasing wavelength, little else is known about the formaldehyde photochemical system. There is no strong evidence concerning the role of the triplet state in the decomposition except that it is formed and does not convert to the ground state by a radiative process.



## Chapter III

### The Calculations on the Formaldehyde System

#### The Equilibrium Geometries and Transition Energies

As there is, then, little information concerning the decomposition of formaldehyde, molecular orbital calculations were performed to evaluate the role of the various states of formaldehyde in its photochemistry. The correlation of various states with products and the nature of the decomposition path was investigated. The results of this study are discussed below.

Calculations were carried out on the various electronic states of formaldehyde to obtain the equilibrium geometries, and the vertical and 0-0 transition energies. The results of the calculations are collected in tables II and III. The calculations were carried out using the CNDO/2 approximation described in chapter I, the coordinate system is described in figure III. They were performed on the triplet and singlet excited states arising via the promotion of one electron, as well as closed shell excited states. The SCF calculations on the singlet states were performed using the method of Kroto and Santry<sup>32</sup>. The programmes used to perform these calculations were supplied by Dr. D. P. Santry.

The equilibrium geometries were calculated by the following method: an initial geometry was used, that of the ground state or some similar excited state or the experimentally measured geometry, then one of the bond

TABLE II

A Comparison of Observed<sup>34</sup> and Calculated Geometries of H<sub>2</sub>CO\*

State		Thet(1) <sup>o</sup>	Thet(2) <sup>o</sup>	PS <sup>o</sup>	R(1)	R(2)	R(3)	Energy Atomic Units
GS	Calc	57.0	57.0	0	1.24	1.117	1.117	-26.8395
	obs.	57.9	57.0	0	1.210	1.102	1.102	
<sup>1</sup> <sub>n,π*</sub>	Calc	62.75	62.75	0	1.31	1.10	1.10	-26.7136
	obs.	59.5	59.5	20.5	1.32	1.092	1.092	
<sup>3</sup> <sub>n,π*</sub>	Calc	58.0	58.0	35.0	1.31	1.11	1.11	-26.7336
	obs.	60.5	60.5	38.0	1.31	1.08	1.08	
<sup>3</sup> <sub>π,π*</sub>	Calc	57.6	57.6	28.0	1.38	1.11	1.11	-26.6527
	obs.							
<sup>3</sup> <sub>n,σ*</sub>	Calc	78.0	78.0	0	1.255	1.30	1.30	-26.5920
	obs.							

\* The Coordinate System is given in Figure III.

TABLE III

A Comparison of Calculated with Observed<sup>34</sup> Transition Energies of H<sub>2</sub>CO

State	Vertical Transitions		0-0 Transitions	
	Calculated	Observed	Calculated	Observed
G. S.	<sup>1</sup> A <sub>1</sub>	0	0	0
<sup>1</sup> (n,π*)	<sup>1</sup> A <sub>2</sub> ( <sup>1</sup> A'')	3.95	3.5 5.4	3.7 3.58
<sup>3</sup> (n,π*)	<sup>3</sup> A( <sup>3</sup> A'')	3.4	3.13 3.44	2.9 3.21
<sup>1</sup> (n,σ*)	<sup>1</sup> B <sub>2</sub>	---	---	---
<sup>3</sup> (n,σ*)	<sup>3</sup> B <sub>2</sub>	7.30	---	6.7 ----
<sup>1</sup> (π,π*)	<sup>1</sup> A <sub>1</sub>	11.5**	---	---
<sup>3</sup> (π,π*)	<sup>3</sup> A <sub>1</sub>	6.76	---	5.1 ----

\*\* obtained from the CI calculation.

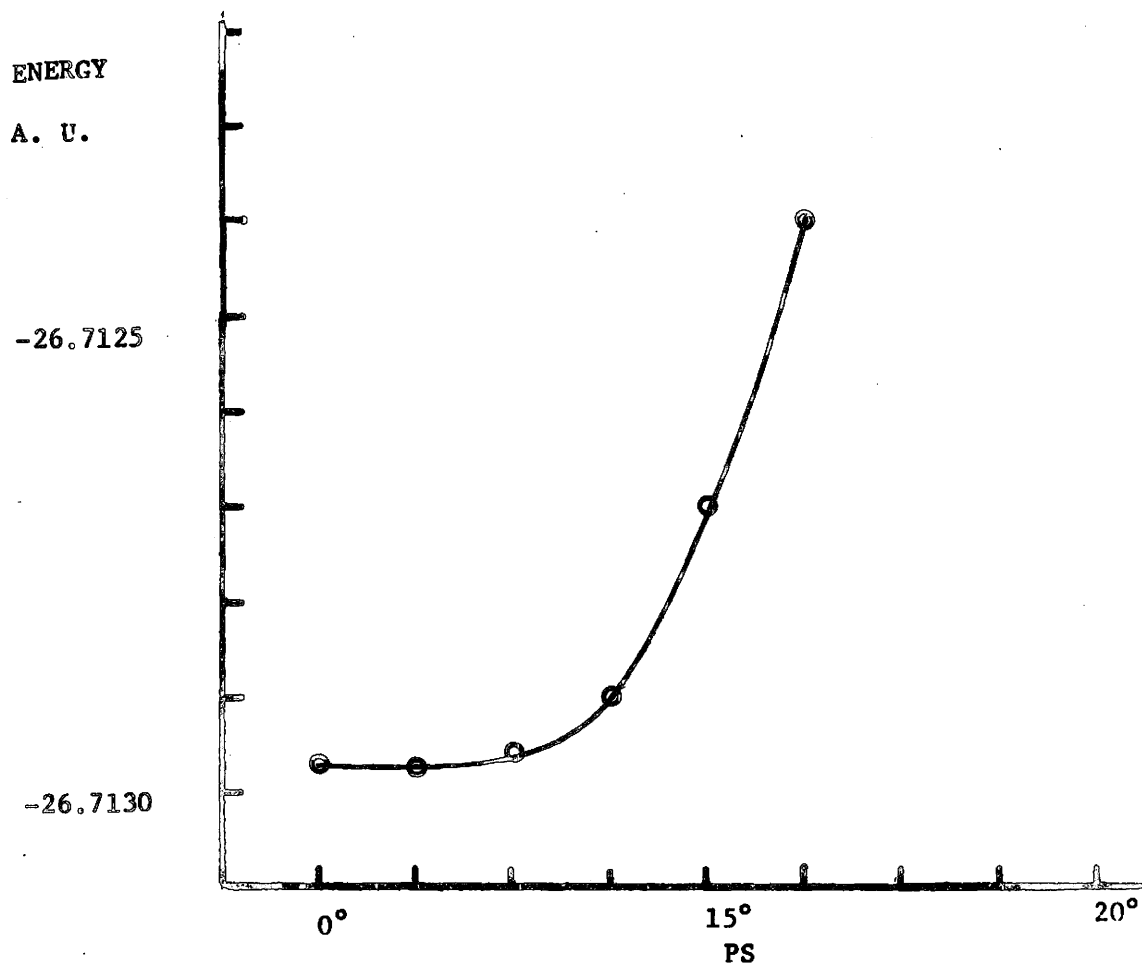
lengths or bond angles was varied until a minimum energy was obtained. This procedure was carried out for all the remaining parameters, one at a time. The cycle was repeated until no significant change occurred.

In general, good agreement is obtained for the calculated geometries and those observed experimentally (see Table II and III). There are two notable exceptions, the carbon oxygen bond length in the ground state and the angle made by the carbon oxygen bond with the carbon hydrogen plane in the  ${}^1A_2({}^1A'')$  state. The poor carbon-oxygen bond length in the ground state seems to be a result of the CNDO approximations<sup>7,32,33</sup>. The contributions to the  $2b_2$  orbital in the ground state, by the carbon and oxygen atomic orbitals are strongly antibonding, (see appendix). In fact, states which arise from depopulation of this orbital give a bond length which agrees more favourably with that observed.

The oxygen out of plane angle for the equilibrium geometry is in error by some  $20^\circ$  (see Table II) and, in fact, gives no barrier to inversion (see above). The calculation does, however, show that the angle can be varied some  $10^\circ$  from planarity with no increase in energy (see Fig. IX). The energy increase upon further changing the angle is quite small (a change of  $20^\circ$  from planarity increases the energy by 0.0003 Au or 0.2 Kcal/mole). Thus, although the calculation doesn't actually show a barrier to inversion, it does reflect the fact that there is very

Figure IV

Variation of the Out of Plane Angle  $P_s$  in the  $1_n, \pi^*$  State



Coordinates:  $R_1 = 1.31 \text{ \AA}$ ;  $R_2 = R_3 = 1.09 \text{ \AA}$ .  $\text{Theta} = 122.0^\circ$

little resistance to motion through the plane. The barrier has been estimated, from spectroscopic data, to be  $650 \text{ cm}^{-1}$  or  $1.85 \text{ kcal/mole}^{18,19}$ .

The energies were calculated of both the 0-0 and vertical transitions for a number of states and are tabulated in Table III. Unfortunately, the energies for the singlet and triplet of the  $n,\pi^*$  states are the only ones which can be compared with the observed values (see preceding discussion on the spectroscopy of formaldehyde) and for these there is good agreement (see Table III).

The singlet excited states were calculated using the method described by Kroto and Santry<sup>32</sup>. The method involved the simultaneous independent calculations on three sets of orbitals, the core orbitals, i.e. those orbitals that are doubly occupied, and the molecular orbitals that were occupied by a single electron. Thus, convergence was somewhat slow and oscillatory. The calculations were also extremely sensitive to geometry in that, at a geometry where two molecular orbitals had similar energies, the program would alternately populate one orbital and then the next, resulting in a divergence. This switching was uncontrollable, and the calculations for the singlet energies of  $n,\sigma^*$  and  $\pi,\pi^*$  states could not be performed. The vertical transition energy quoted for the  $\pi,\pi^*$  state, in Table III was obtained from the configuration interaction calculation which is described below.

There is reasonable agreement between the values calculated in this study and those reported by other

researchers (see Table IV), the one exception being the transition energy for the  $^3n,\sigma^*$  state. The value obtained is somewhat lower than that reported by Beunker and Peyerimhoff<sup>33</sup>. This is due to the fact that, while the value quoted in this study was obtained by a single SCF calculation, that of Beunker and Peyerimhoff<sup>33</sup> was the result of a detailed Configuration Interaction calculation. It should be noted that the transition energy calculated for the  $^1\pi,\pi^*$  state based on a simple C.I. calculation agrees extremely well (11.55 ev vs. 11.72 ev) with Beunker's value.

TABLE IV

## Transition Energies (ev)

## A Comparison of Various Calculations of the Transition Energies

		0-0 Transitions						
State		Bene <sup>35</sup>	Geuisner <sup>36</sup>		Beunker <sup>33</sup>	Whitter <sup>38</sup>	This Study	
		& Jaffe	Pretre & Pullman	Segal <sup>37</sup>	& Peyerimhoff	& Hackmeyer		
			CIS	CISD				
<sup>1</sup> (n,π*)	( <sup>1</sup> A <sub>2</sub> ) <sup>1</sup> A''	3.4	4.61	5.45			3.7	
<sup>3</sup> (n,π*)	( <sup>3</sup> A <sub>2</sub> ) <sup>2</sup> A''	---	5.02	5.45			2.9	
<sup>1</sup> (n,σ*)	<sup>1</sup> B <sub>2</sub>	---	11.27	9.83			---	
<sup>3</sup> (n,σ*)	<sup>3</sup> B <sub>2</sub>	---	----	----			6.7	
<sup>1</sup> (π,π*)	( <sup>1</sup> A <sub>2</sub> ) <sup>1</sup> A'	9.3	11.44	----			---	
<sup>3</sup> (π,π*)	( <sup>3</sup> A <sub>1</sub> ) <sup>3</sup> A'	---	7.63	8.54			5.1	
Vertical Transitions								
<sup>1</sup> (n,π*)	( <sup>1</sup> A <sub>2</sub> ) <sup>1</sup> A''				3.83 ev	3.43 ev	3.80	3.95
<sup>3</sup> (n,π*)	( <sup>3</sup> A <sub>2</sub> ) <sup>3</sup> A''				3.46	3.01	3.38	3.4
<sup>1</sup> (n,σ*)	<sup>1</sup> B <sub>2</sub>				8.12	10.44	----	----
<sup>3</sup> (n,σ*)	<sup>3</sup> B <sub>2</sub>				----	9.55	----	7.3
<sup>1</sup> (π,π*)	( <sup>1</sup> A <sub>1</sub> ) <sup>1</sup> A'				15.6	11.72	11.31	11.5*
<sup>3</sup> (π,π*)	( <sup>3</sup> A <sub>1</sub> ) <sup>3</sup> A'				----	4.99	5.66	6.76

\* from the CI calculation



### The Photodecomposition to Molecular Products

The decomposition products,  $H_2$  and CO, appear to arise via two different pathways, that is, via a direct molecular split and a split into the radical products H and HCO. An attempt to determine the path leading to a particular product demands a knowledge of the states which will give rise to these products, i.e., what state or states would result if formaldehyde were to be formed from the products. This information can be obtained from the Wigner-Witmer correlation rules<sup>18</sup>. The application of the correlation rules will yield a list of states that leads to a particular set of products. However, they will only be identified in so far as the multiplicity and symmetry are specified.

The Wigner-Witmer rules were applied to both the radical products and the molecular products of the decomposition, and the results are shown in the Fig. XIII. There is only one state giving rise to the molecular split, which is a singlet state,  $^1A_1$  if the molecule retains  $C_{2v}$  symmetry throughout the reaction, and  $^1A'$  if the path involves a distortion of the molecule to  $C_s$  symmetry.

Inspection of the virtual orbitals of the ground state (see appendix) shows that the  $4a_1$  orbital has characteristics which would lead to a molecular split. The orbital is bonding between the two hydrogen atoms, and the carbon and oxygen atoms, while being strongly antibonding between the carbon and two hydrogen atoms. Thus, it would seem reasonable that if this orbital were doubly occupied at the expense of another orbital,

the  $2b_2$  non-bonding orbital, this state would lead to the correct products.

To test this hypotheses, a calculation was performed, using a closed shell CNDO/2 program, on this  $n^2, \sigma^*2$  state, which is  $^1A_1$ . This electronic configuration was specified as the molecule was distorted along a  $C_{2v}$  path, that is, the two hydrogen atoms were drawn away from the carbon centre symmetrically about the C=O axis, while maintaining planarity. The energy for the optimum configuration for a particular C-H distance was found to decrease as the C-H distance increased. Also the optimum geometry tended toward a smaller H-C-H angle as the C-H distance increased.

The carbon oxygen bond distance in formaldehyde was specified as that in the carbon monoxide molecule in its ground state. The equilibrium geometry of carbon monoxide was calculated using the same computer programme as for the formaldehyde calculations. The energy of the formaldehyde was then studied as a function of hydrogen-hydrogen distance and carbon hydrogen distance, and the energy was found to smoothly approach a value equal to the sum of the electronic energies of an isolated carbon monoxide and hydrogen molecule, both in the ground state (see Table V and Figures V-X). That this was, in fact, the lowest energy state was tested by specifying the lowest energy molecular orbitals to be occupied, irrespective of symmetry. The same configuration resulted.

Thus, it is clear that the SCF state  $n^2, \sigma^*2$  leads to the correct products, that is carbon monoxide and hydrogen

TABLE V

Energies of Decomposition Products of  $\text{H}_2\text{CO}^1(n^2, \sigma^*2)$ 

Molecule	Energy	Equilib. Geom.
	at equilib. Geom.	
CO	25.0621 Au	1.191 Å
H <sub>2</sub>	1.47465 Au	0.75 Å
Total H <sub>2</sub> + CO	26.53675 Au	-----
H <sub>2</sub> CO <sup>1</sup> (n <sup>2</sup> ,σ* <sup>2</sup> )	26.5368 Au	RC = O 1.191 Å
		R CH 2.6 Å
		RH-H .74 Å

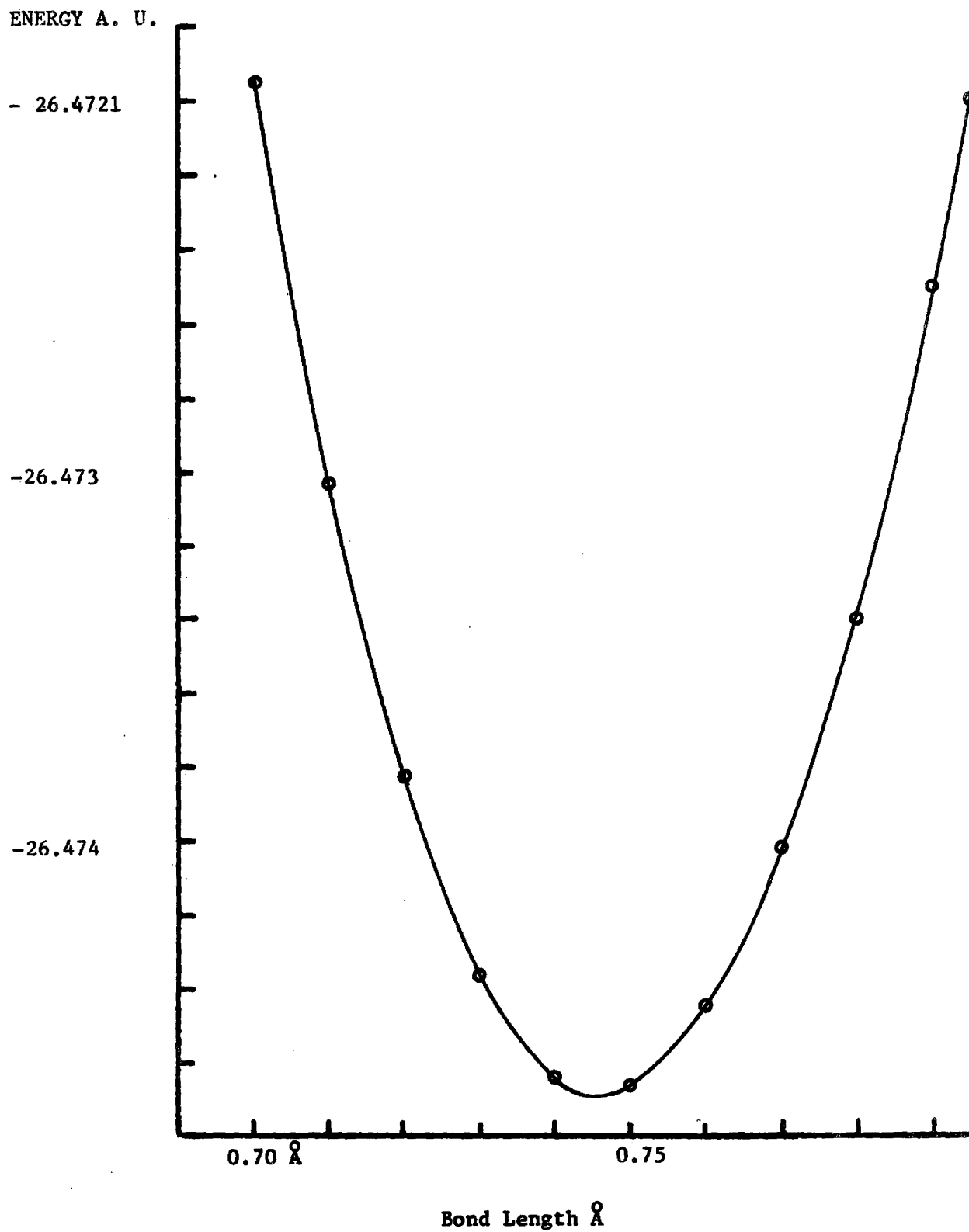
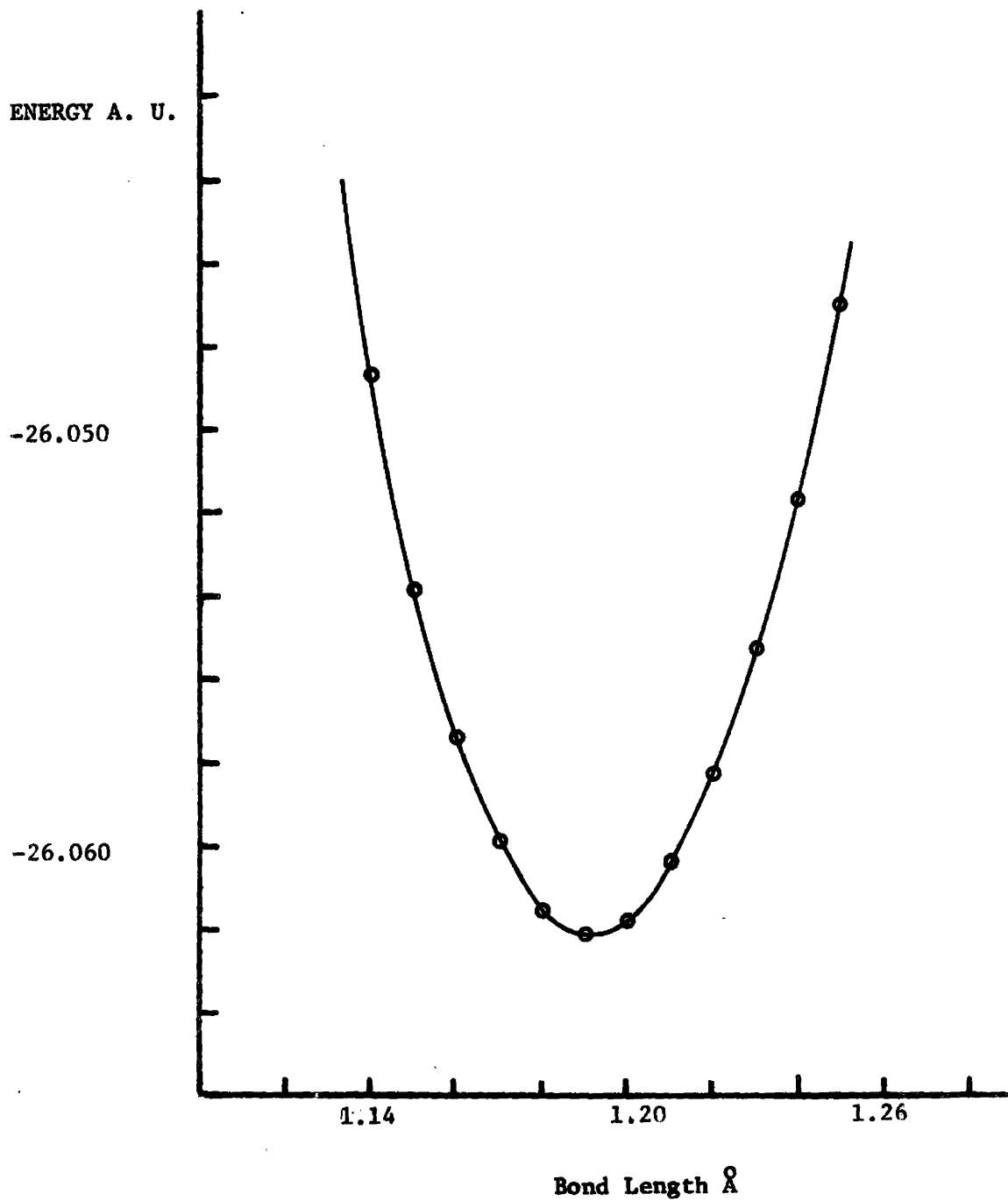


Figure V: The Energy of  $H_2$  vs. Bond Length (Ground State)

Figure VI: The Energy of CO vs. Bond Length (Ground State)



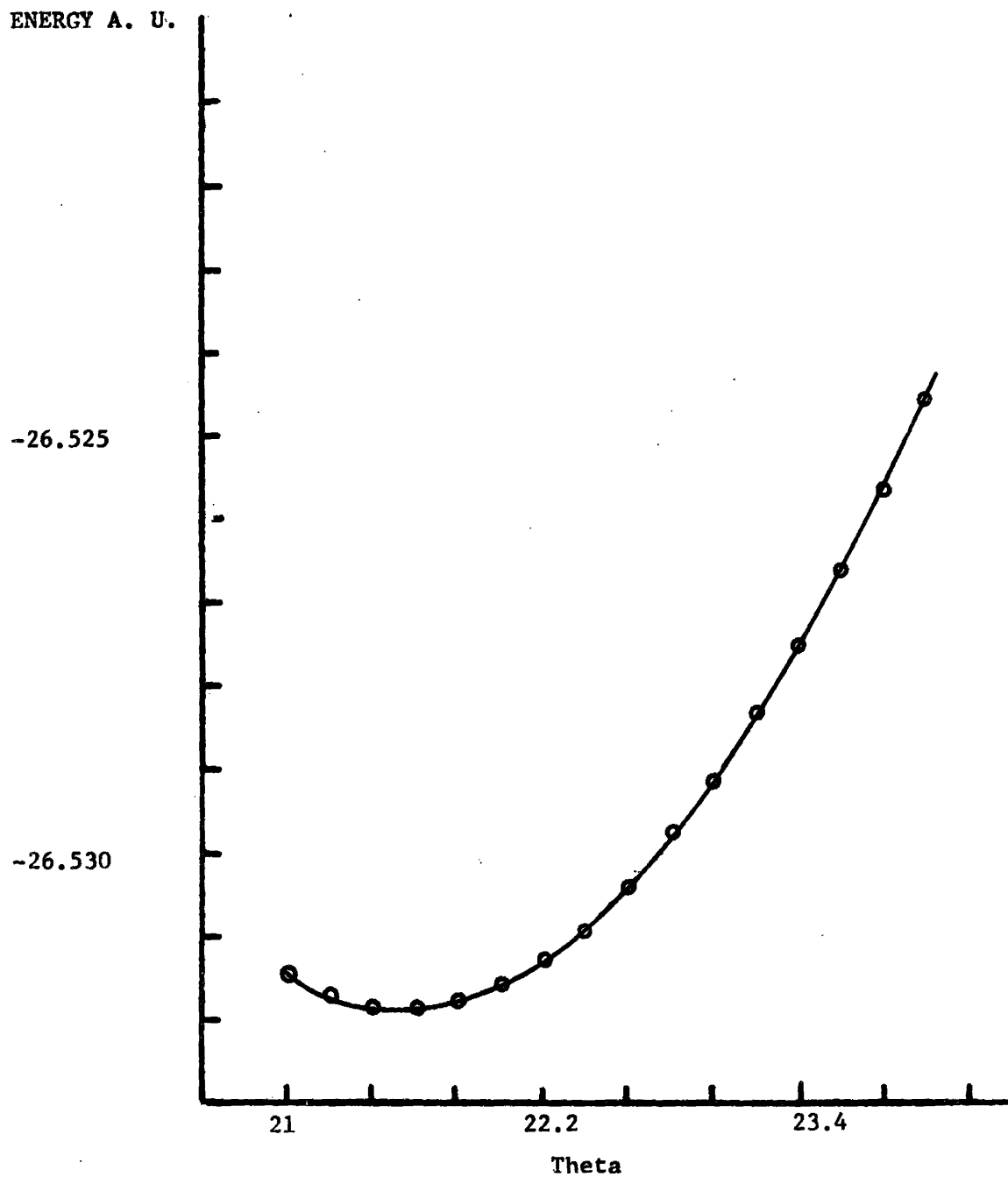
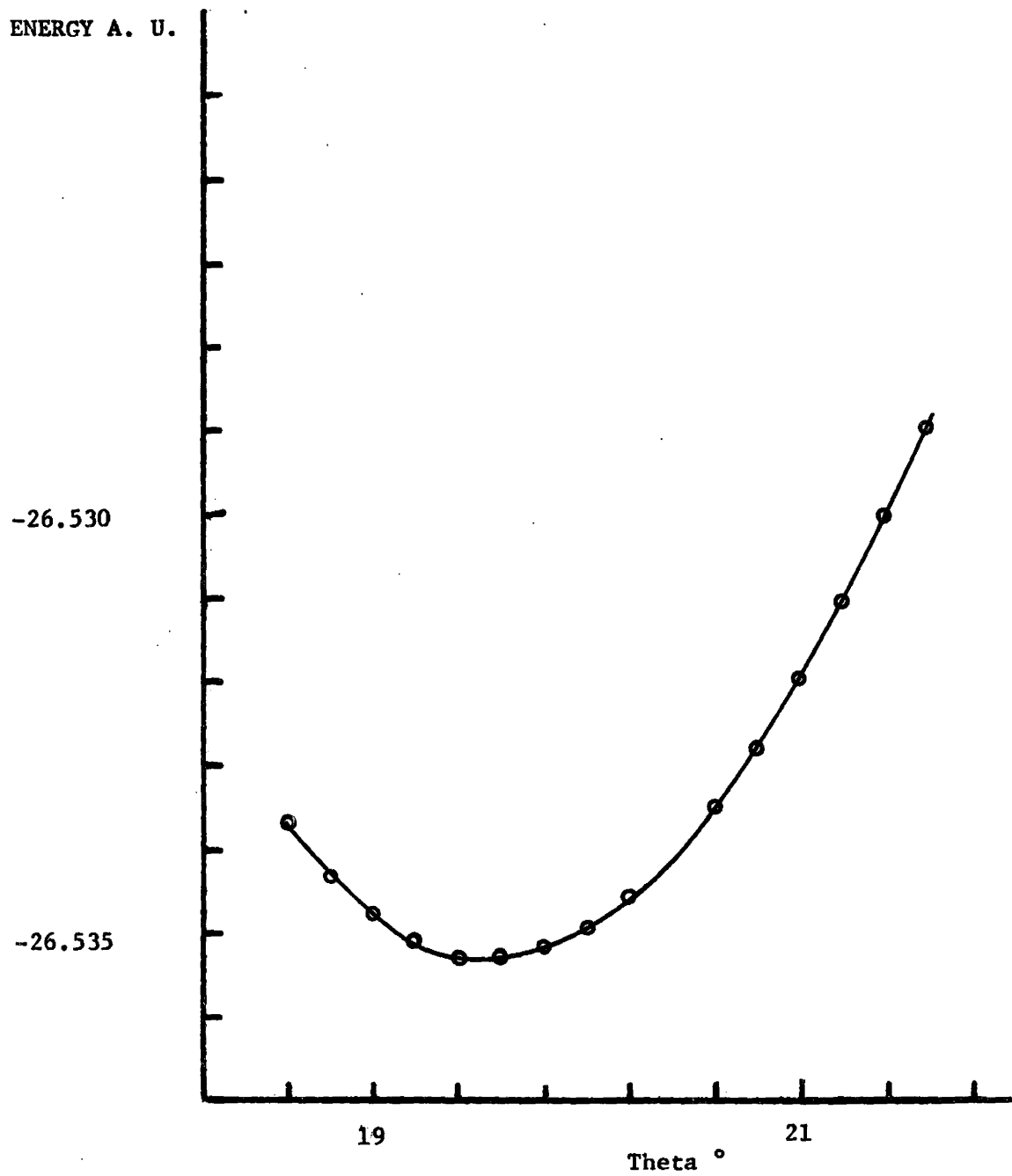


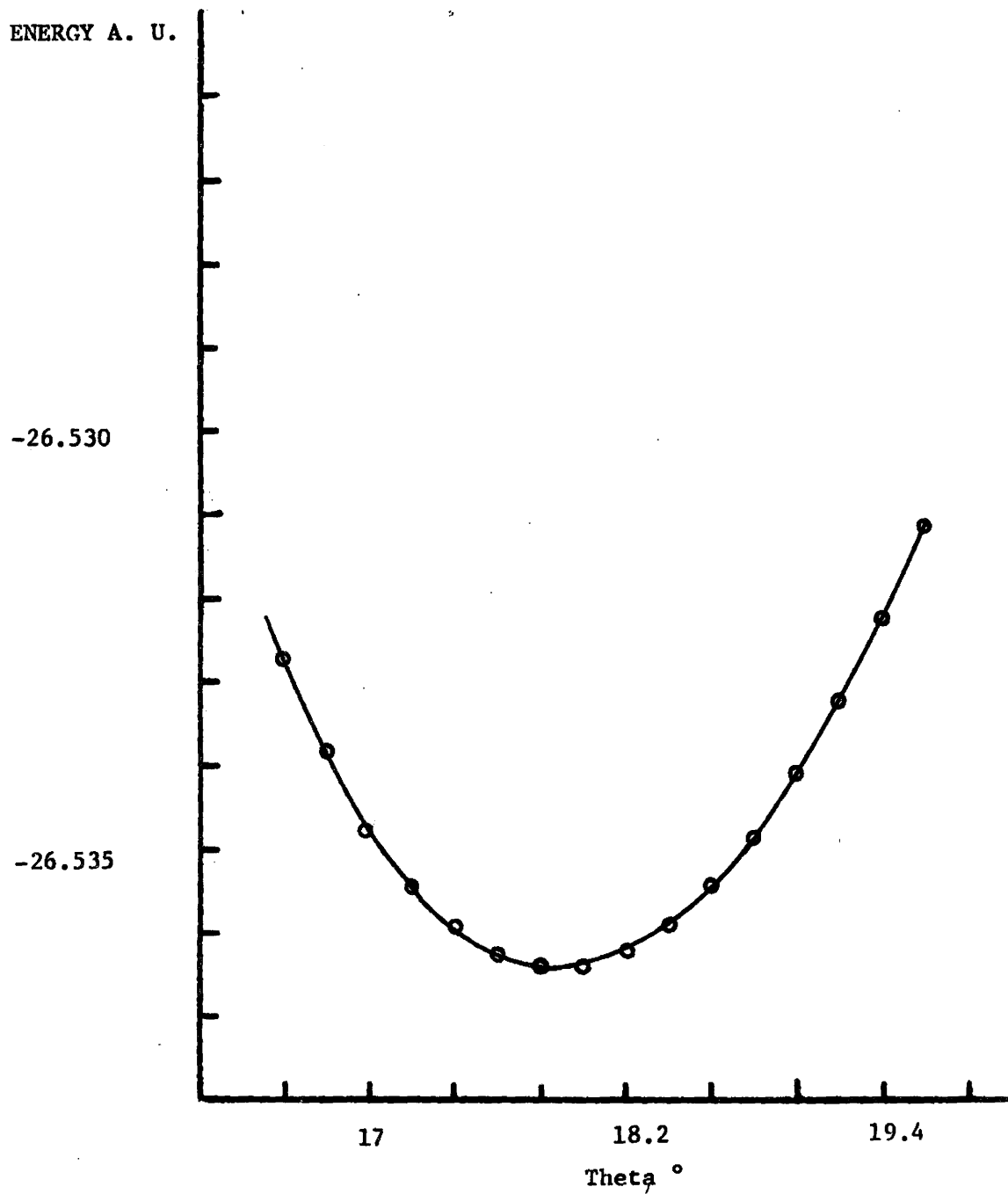
Figure VII: The Energy of  $\text{H}_2\text{CO}$  vs. Theta:  $n^2, \sigma^{*2}$  State.

Coordinates:  $R_1 = 1.193$ ;  $R_2 = R_3 = 2.0 \text{ \AA}$

Figure VIII: Energy of  $\text{H}_2\text{CO}$  vs. Theta:  $n^2, \sigma^{*2}$  State



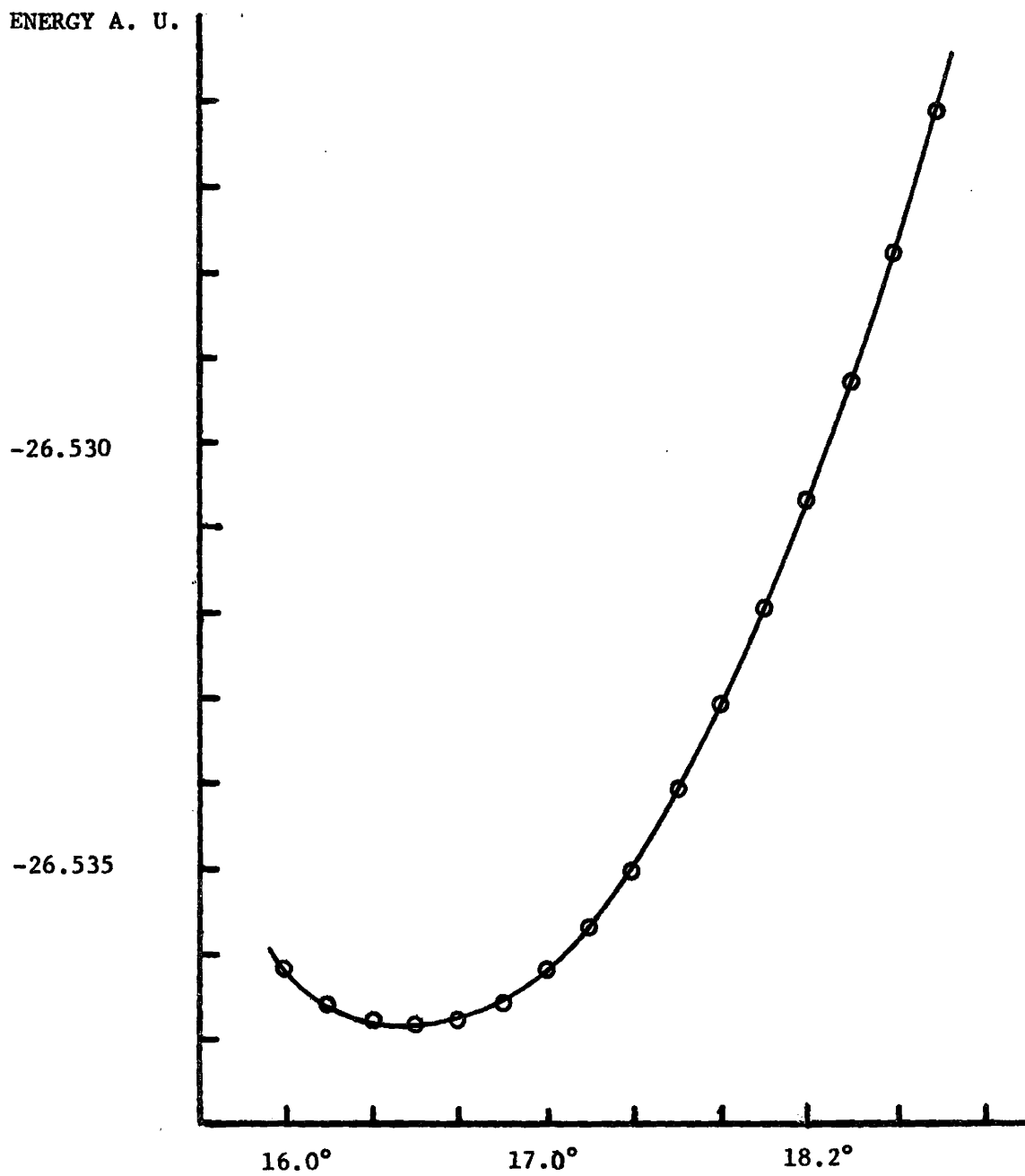
Coordinates:  $R_1 = 1.191 \text{ \AA}$ ;  $R_2 = R_3 = 2.2 \text{ \AA}$ .

Figure IX: Energy of  $\text{H}_2\text{CO}$  vs. Theta  $n^2, \sigma^{*2}$  State

Coordinates:  $R_1 = 1.191 \text{ \AA}$ ;  $R_2 = R_3 = 2.4 \text{ \AA}$



Figure X: Energy of  $\text{H}_2\text{CO}$  vs. Theta  $n^2, \sigma^{*2}$  State



Coordinates:  $R_1 = 1.191 \text{ \AA}$ ;  $R_2 = R_3 = 2.6 \text{ \AA}$ .

molecules in their ground electronic states. However, it is to be noted that  $\text{CO}$  and  $\text{H}_2$  are the lowest energy products, and, in fact, have virtually the same energy as ground state formaldehyde: the products have an energy of 1.3 kcal relative to that of ground state formaldehyde<sup>16</sup>. Thus, the dissociative surface of the  $n^2, \sigma^{*2}$  state must cross that of the ground state. Since the ground state is also  $^1A_1$ , this is prohibited by the non-crossing rule.

Thus, while the non-crossing rule appears to prohibit the  $n^2, \sigma^{*2}$  state from correlating with the ground state products, i.e. the molecular products of the dissociations, the configuration of the state at large carbon hydrogen bond lengths is that of isolated carbon monoxide and hydrogen molecules. That state which will give rise to these products must, then, acquire a similar configuration. This assumption is reasonable as the extent to which one configuration mixes with another depends upon the energy difference between the states (see above), which is dependent upon the geometry. Thus, as the molecule in its ground state is distorted along the path leading to molecular products, the CI description of the state will contain a greater contribution from the  $n^2, \sigma^{*2}$  state. Thus, it can be expected that the ground state of formaldehyde will look very much like the SCF description of the  $n^2, \sigma^{*2}$  state as the molecule begins to form the products  $\text{CO}$  and  $\text{H}_2$ .

The CI calculation performed was done as follows: the interacting states were constructed from the virtual orbitals of the ground state by exciting one or two electrons from the occupied orbitals into a virtual orbital. All  $^1A_1$  states

involving the excitation of one electron, and all closed shell states arising from the excitation of two electrons were included in the interaction matrix. The details of the calculation have been described above.

The calculated surface (see Figs. XI and XII) shows the variation in the potential energy of the formaldehyde molecule as a function of the coordinates of the two hydrogen atoms. The coordinates of the hydrogen atoms are varied with the restriction that the molecule remain planar and retain  $C_{2v}$  symmetry. The carbon-oxygen bond length chosen was 1.24 Å.

The surface was constructed by plotting equal energy contours as a function of hydrogen-hydrogen (H-H) bond distance and carbon to the centre of the hydrogen-hydrogen bond distance ( $C_{\perp}HH$ ). These contours were obtained from plots of (H-H) distance versus potential energy for particular values of the ( $C_{\perp}HH$ ) distance and vice versa.

### The Reaction Surface

The surface has been constructed in two sections, for reasons given below (see Figures XI, XII). The first section makes use of the virtual orbitals of the ground state, i.e., the SCF state having the configuration  $(1a_1)^2(2a_1)^2(1b_2)^2(3a_1)^2(1b_1)^2(2b_2)^2$ . The ground state, at the equilibrium geometry is described almost exclusively as the SCF ground state, the coefficient of mixing being 0.982. The second section makes use of the SCF state  $n^2, \sigma^{*2}$  as the ground state, that is the configuration  $..(1b_1)^2(2a_1)^2$ . The coefficient of mixing of this state to the ground state is 0.987, for a set of coordinates corresponding to a carbon monoxide molecule at a distance of

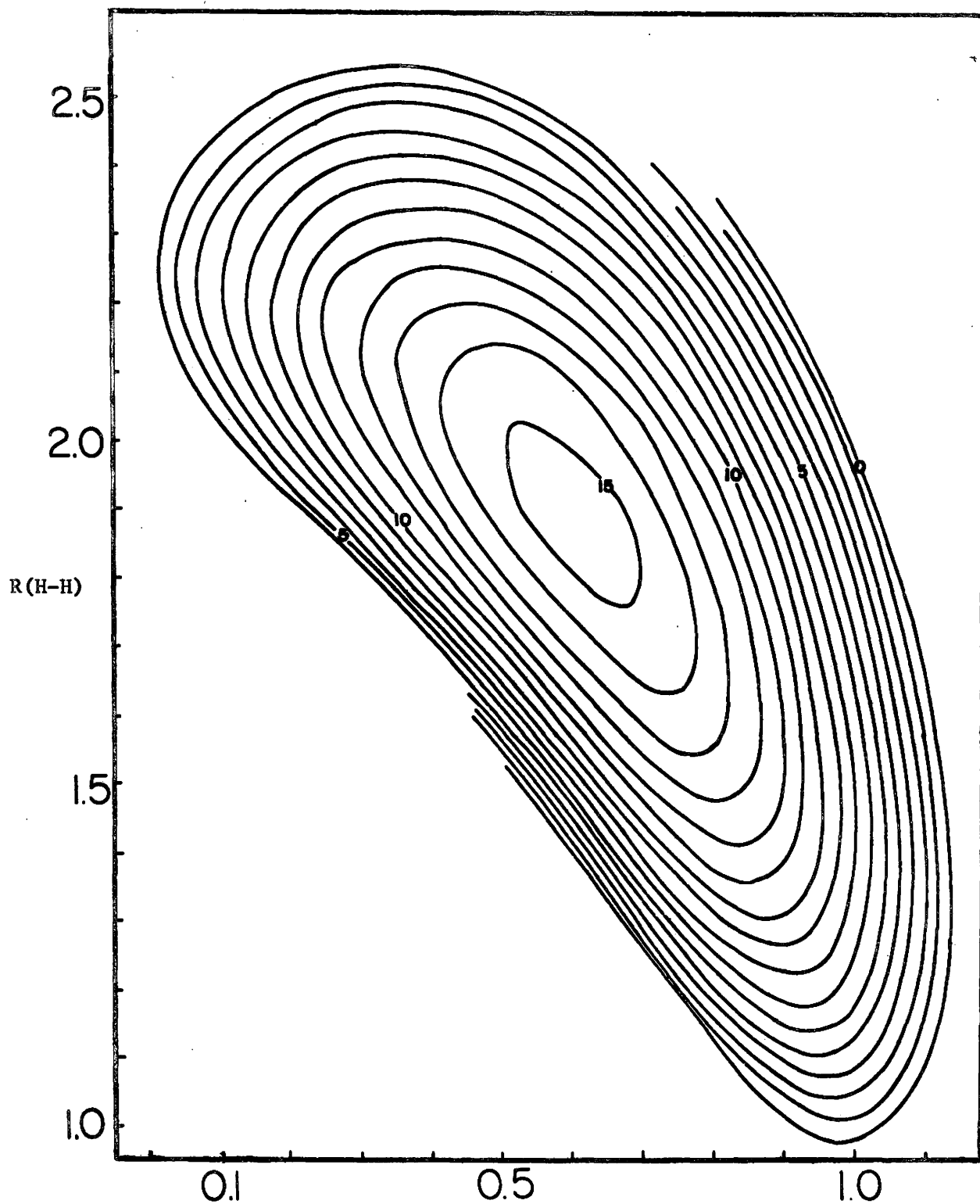


Figure XI: Potential Energy Surface for Ground State Formaldehyde Part A. Energy plotted in units of 0.01 A.U. as a function of H-H distance ( $R(H-H)$ ) and Carbon to centre of H-H bond distance ( $R(C-HH)$ ). The molecule maintains  $C_{2v}$  symmetry, and the occupancy is the lowest energy orbitals. They are the following:  $3(a_1)^2$ ,  $1(b_1)^2$ ,  $2(b_2)^2$ .

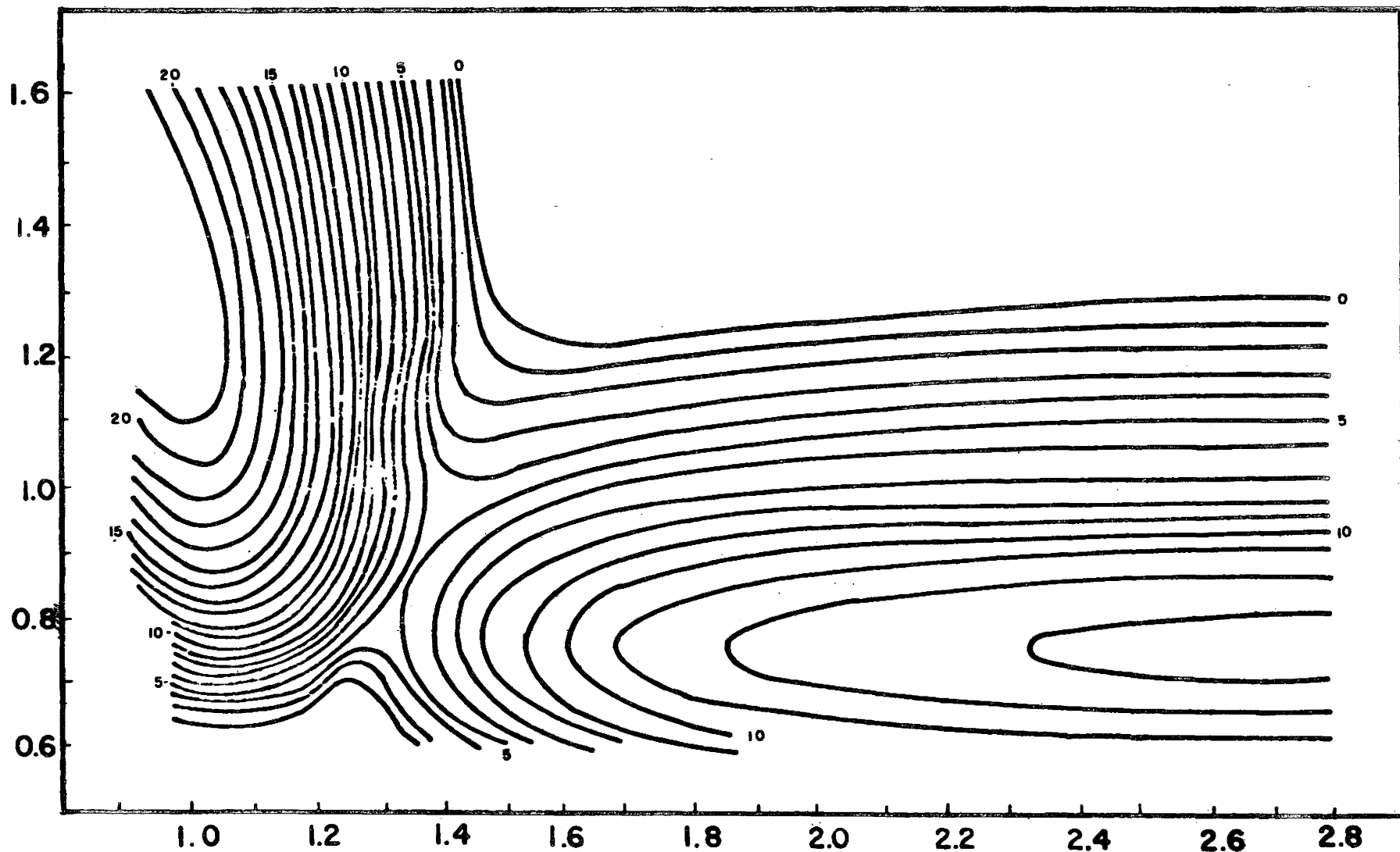


Figure XII: Potential Energy Surface for Ground State Formaldehyde Part B. Energy plotted in units of 0.01 A.U. as a function of H-H distance (R H-H) and Carbon to centre of H-H bond distance (R C HH). The molecule maintains  $C_{2v}$  symmetry, and the occupancy is the lowest energy orbitals. They are the following:  $3(a_1)^2$ ,  $1(b_1)^2$ ,  $2(b_2)^2$ .

3Å from a hydrogen molecule.

As the molecule travelled a path toward dissociation into molecular products, the mixing coefficient of the ground state in the CI description of the  $\pi^2, \sigma^{*2}$  state and vice versa approached equality. As the coefficients approached each other, the difference in energies between the two states became first smaller and then began to diverge. This is a consequence of the non-crossing rule. As two states of the same symmetry approach each other in energy as they follow a particular coordinate in n-dimensional space, they must begin to repel each other, and the states must diverge.

When performing a calculation of this type there are two aspects which must be considered. The first is that, as a result of the approximate methods used, the energies of two molecules cannot be compared. Thus, the calculated energy of the formaldehyde molecule, in its ground state cannot be compared with the energy of the molecular fragments for molecular hydrogen and carbon monoxide. In this case the energy of the molecular product is calculated to be far higher than the energy of ground state formaldehyde when, in fact, they are almost equal. This effect will result in a potential energy surface in which the energy change along a potential path to products will be superimposed upon the inherent energy increase on the molecules moving on the path tends towards the fragments.

As has been mentioned earlier, this type of calculation can be sensitive to geometry. Thus, specification of a particular electronic configuration can lead to oscillations for particular geometries, usually when the molecule is distorted

from its equilibrium geometry for this configuration.

As a result, the surface could not be calculated in its entirety by specifying the same electronic configuration for the SCF states whose orbitals are used to construct the virtual states of the interaction matrix. Thus, when the energies of the ground state and the  $n^2, \sigma^{*2}$  state crossed, the state with the lower energy was used as the SCF state. The virtual states used in the interaction matrix were constructed by the excitation of one or two electrons from an occupied orbital and placing them in a virtual orbital. By changing the configurations of the SCF state, then, many of the states previously calculated disappeared from the matrix as they would involve three and four electron excitations, and were replaced by others. This results in a difference in the CI matrix and is reflected in a change of energy in the CI ground state. As a result, there is a discontinuity in the surface, and the surface is constructed in two parts. This could be overcome by using a complete interaction matrix involving all possible  $^1A_1$  states, but, it is the shape of the surface which is of interest, not the absolute magnitude of the energies. In the region where both "halves" of the potential surface overlap it is seen that the contours are of the same shape and direction, apparently only differing in energy.

The surface is typical of what is expected for a stable molecule such as formaldehyde. The contours of the surface are plotted 0.01 au (0.21 ev) apart and form closed loops about the equilibrium geometry of the molecule, the contour being oval shaped. Inspection of the surface show that for any extension of the (C $\underline{L}$ HH) bond lengths, the energy required is

lowered by decreasing the (H-H) bond distance. This trend continues until the maximum of the reaction surface is reached, and "X" shaped region from which the energy falls off sharply as the (C<sub>1</sub>H<sub>2</sub>H) distance is increased.

At a (C<sub>1</sub>H<sub>2</sub>H) bond length of about 1.4 Å the surface falls away sharply along a constant (H-H) bond distance to products. The surface becomes, at a distance of 2 Å essentially that of a hydrogen molecule, the energy being independent of the (C<sub>1</sub>H<sub>2</sub>H) distance.

To construct the surface, a number of constraints had to be placed on the dissociative mechanism: the molecule remains planar throughout the dissociation, the path retains symmetry about the carbon-oxygen axis and the carbon oxygen bond length remains constant, at 1.24 Å. This was done to reduce the number of variables so that a three dimensional surface could be plotted.

The carbon oxygen bond length will undoubtedly change throughout the dissociation. Thus, the surface will be somewhat distorted because of it. That the molecule would remain planar is not known, but it is doubtful that there would be any energy decrease in becoming non-planar.

The energy contours, in the region of very short (C<sub>1</sub>H<sub>2</sub>H) distance and larger (H-H) distance, are quite widely spaced, the surface being somewhat shallow in this region.

The surface could be plotted for negative coordinates, and one might suppose that the interaction of the hydrogen atoms with the orbitals of the oxygen atom would lower the energy barrier to dissociation to the molecular products.



Figure XII shows that this supposition is incorrect and that the energy rises quite steeply for motion in this direction. While this orbital energy is lowered, the nuclear repulsion energy rises quite sharply and the overall effect is a sharp rise in energy.

The result of the calculation indicates that the molecular products, hydrogen and carbon monoxide in their ground states, arise via the decomposition of the formaldehyde ground electronic state. The path followed in this decomposition is a lengthening of the carbon hydrogen bond length accompanied by the simultaneous shortening of the hydrogen hydrogen bond length. This path is, in fact, either the  $\nu_2(a_1)$  or  $\nu_3(a_1)$  normal mode of formaldehyde or is a combination of both. The motion of the carbon-oxygen bond was not investigated, in part because of the obvious difficulty in constructing four dimensional surfaces.

#### The Photodecomposition to Radical Products

The process leading to the radical products was also investigated, calculations being carried out using the open shell version of the CNDO/2 programs. The radical products of the dissociation are the formyl radical and the hydrogen atom, the hydrogen atom being in its ground state since the lowest excited state of the hydrogen atom lies well above the  $^1n,\pi^*$  state of formaldehyde.

Calculations were carried out on the formyl radical to determine the ground state geometry, the results are tabulated below (Table VI). The formyl radical, in the linear configuration is a member of the  $C_{\infty v}$  point group. Occupation of the lowest lying orbitals results in two  $\pi$  and two  $\Sigma$  orbitals

Table VI**Equilibrium Geometries and Transition Energies of Two States of HCO**

State		RCO	RCH	Theta	Transitions	
$^2A'$ (G.S.)	Calc	1.22	1.11	46°	0-0	Vert.
	obs. <sup>18</sup>	1.14	1.08	60.5°	---	----
$^2A''$	Calc	1.22	1.11	0°	1.14 ev.	----
	obs. <sup>18</sup>	1.187	1.04	0°	1.33 ev.	1.16 - 5.7

being doubly occupied, and one  $\pi^*$  orbital being singly occupied; the state being  ${}^2\pi$ , which is doubly degenerate. The degeneracy is lifted by bending the molecule, the occupancy being three  $(a')^2$ , one  $(a'')^2$  and one  $(a''')$  or three  $(a')^2$ , one  $(a'')^2$  and one  $(a')$ , and the latter configuration is the lowest in energy a  ${}^2A'$  state, and the former a  ${}^2A''$  state.

The difference in energy between these two states is quite small, the 0-0 transition being  $1.33 \text{ eV}^{18}$ . Because of this small energy difference, the two states of the formyl radical must be considered as possible dissociation products.

The reaction path must be specified before the Wigner-Witmer<sup>18</sup> rules can be applied, and the species must be treated as belonging to the point group of the least symmetric species present. Thus, if the intermediate configuration is of lower symmetry than any of the reactants or products, the Wigner-Witmer rules are applied as if each species were a member of that group. If a planar reaction path is specified, the states which correlate with products will be those specified in Figure XIII.

The Wigner-Witmer<sup>18</sup> rules specify only the spin and symmetry of the state which correlates with a particular state of a given symmetry. The non-crossing rule, however, specifies that the lowest state of a particular symmetry correlates with the lowest energy products, corresponding to a state of that symmetry. Thus, the states which correlate with particular products are listed in Figure XIII.

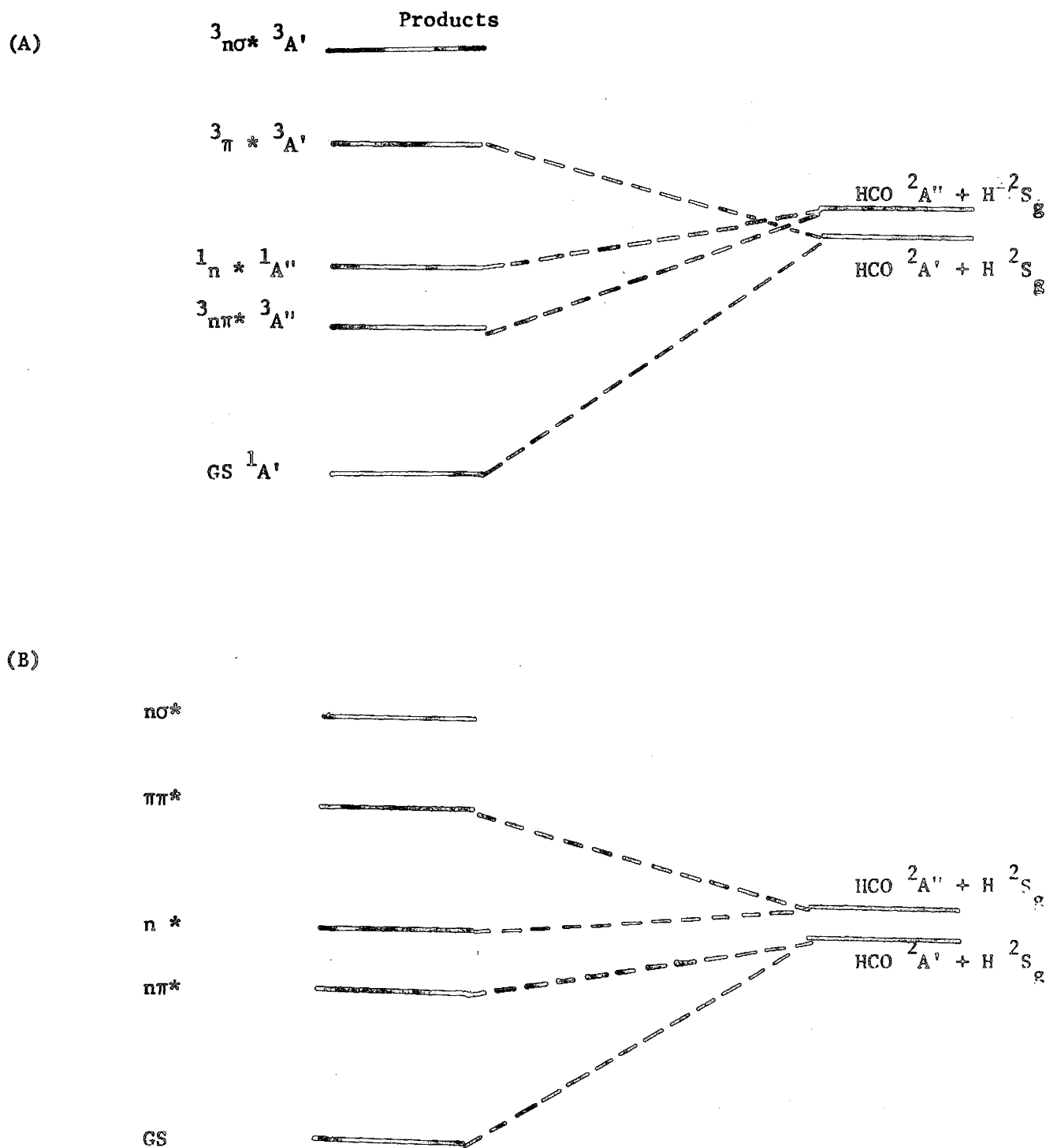
Inspection of the virtual orbitals of the ground state indicates an  $n, \pi^*$  state would correlate with the ground state products  $\text{HCO } 2A'$  and  $\text{H}^2\text{S}_2$ . Calculations were performed

on this state to determine whether it correlates smoothly with ground state products. The restriction placed on the path of decomposition was that the molecule remain planar, that is, retains at least  $C_s$  symmetry.

The calculations were carried out using an open shell version of the CNDO/2 programs. Only the triplet state was investigated as, for reasons given above, the singlet state calculations were too unstable for distorted geometries. The calculation was performed in an unrestricted manner, that is, the orbitals of the  $\alpha$  electrons were allowed to differ from the orbitals of the  $\beta$  electrons and the  $m_s = \pm 1$  component of the triplet was investigated. The state was specified by occupying three  $a'$  and one  $a''$   $\alpha$  orbitals, and five  $a'$  and one  $a''$   $\beta$  orbitals, also specifying that these be the lowest energy orbitals. It was found that this configuration went smoothly to the products in their ground state.

Calculations were performed for a set of coordinates which corresponded to a formyl radical at equilibrium geometry with a hydrogen atom at a distance of  $3\text{\AA}$  from the carbon atom in the plane of the molecule, and on the opposite side of the molecule from the formyl hydrogen. The configuration was not specified beyond occupying the four lowest  $\alpha$  orbitals and the six lowest  $\beta$  orbitals. The configuration resulting was that corresponding to the  $n, \sigma^*$  state, and the orbitals involved were those occupied in the formyl radical plus one other orbital, corresponding to the  $\sigma^*$  orbital.

The path followed by the molecule on dissociation was investigated. The formyl radical was investigated with

Figure XIII: The Correlation of States of  $\text{H}_2\text{CO}$  and  $(\text{CH}_3)_2\text{CO}$  with Radical

A: For a Reaction Path Remaining  $C_s$  Symmetric.

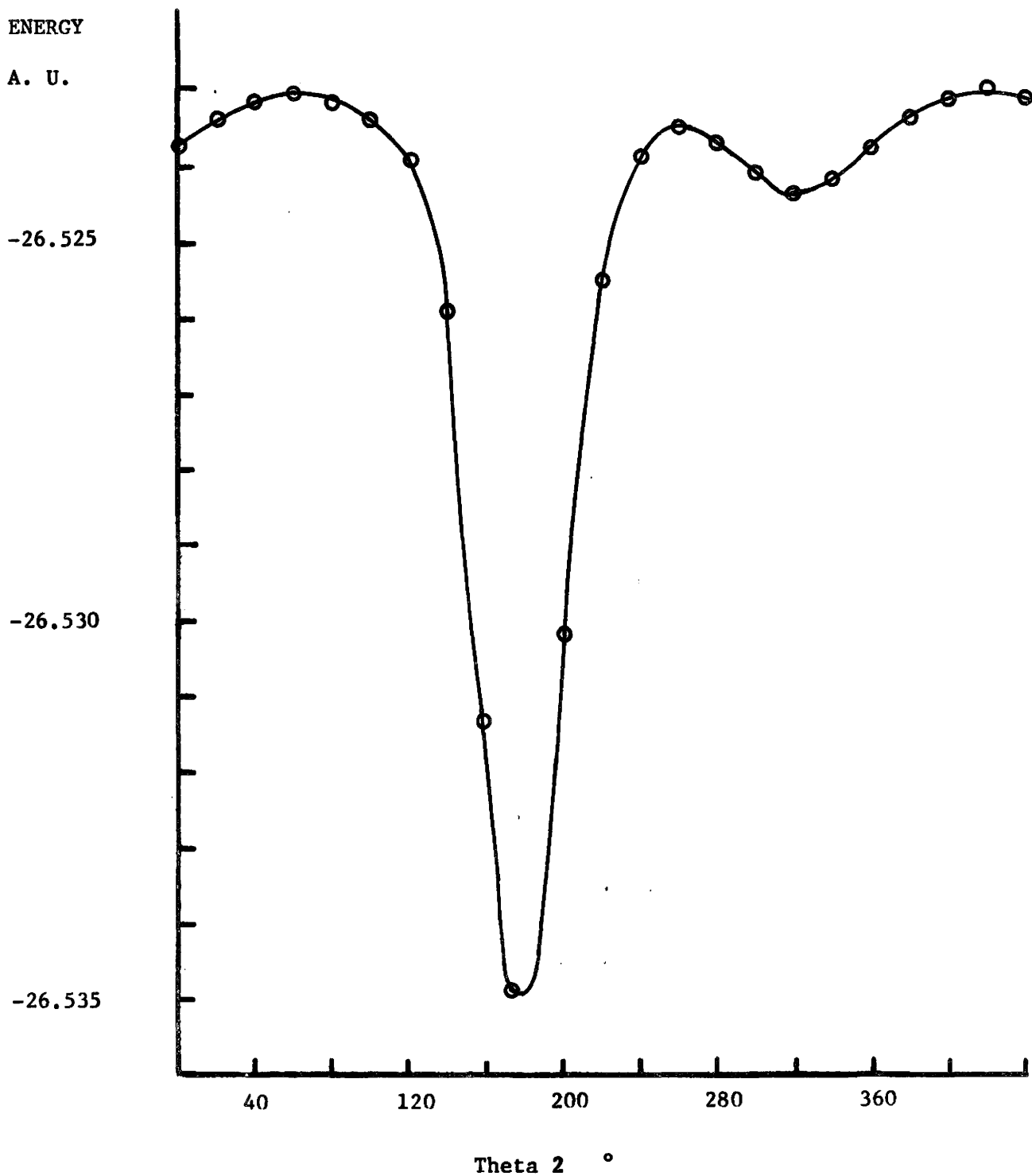
B: For a Reaction Path Passing Through an Intermediate of  $C_1$  Symmetry.

a hydrogen atom at a distance of  $3 \text{ \AA}$ . The angle the hydrogen atom made with the carbon oxygen axis was plotted as a function of energy. (See Fig. XIV) The minimum energy position was found to correspond to a geometry in which the carbon oxygen hydrogen formed a straight line. As the distance from the carbon decreased, the minimum energy geometry was attained at a decreased H-C-O angle. (See Fig. XV) Thus, the hydrogen atom seems to "roll off", that is, as the hydrogen-carbon bond length increases, the bond angle also increases. This means that the molecule is being stabilized by increasing the oxygen-hydrogen overlap. Thus, it is reasonable to assume further stabilization of the energy will be attained by involving a pyramidal or non-planar reaction path which involves more interaction between the p orbitals on the oxygen with the hydrogen 1s orbital.

It was found that the lowest energy configuration was three  $a' \alpha$  one  $a'' \alpha$  five  $a' \beta$  one  $a'' \beta$  until the carbon-hydrogen distance decreased to  $2 \text{ \AA}$ . The configuration giving the lowest energy became three  $a' \alpha$  one  $a'' \alpha$  four  $a' \beta$  two  $a'' \beta$ , that is the  $n, \pi^*$  configuration. Thus, the two states cross at a point very close to products, and it seems reasonable, then, that the  $n, \pi^*$  configuration correlates with the excited state product  $\text{HCO } ^2\text{A} + \text{H } ^2\text{Sg}$ .

The fact that the Wigner-Witmer rules combined with the non-crossing rule specify the  $^3_{\pi, \pi^*}$  state as the one correlating with ground state products as opposed to the  $^3_{n, \sigma^*}$  state is not at odds with the calculation. The configuration  $n, \sigma^*$  is

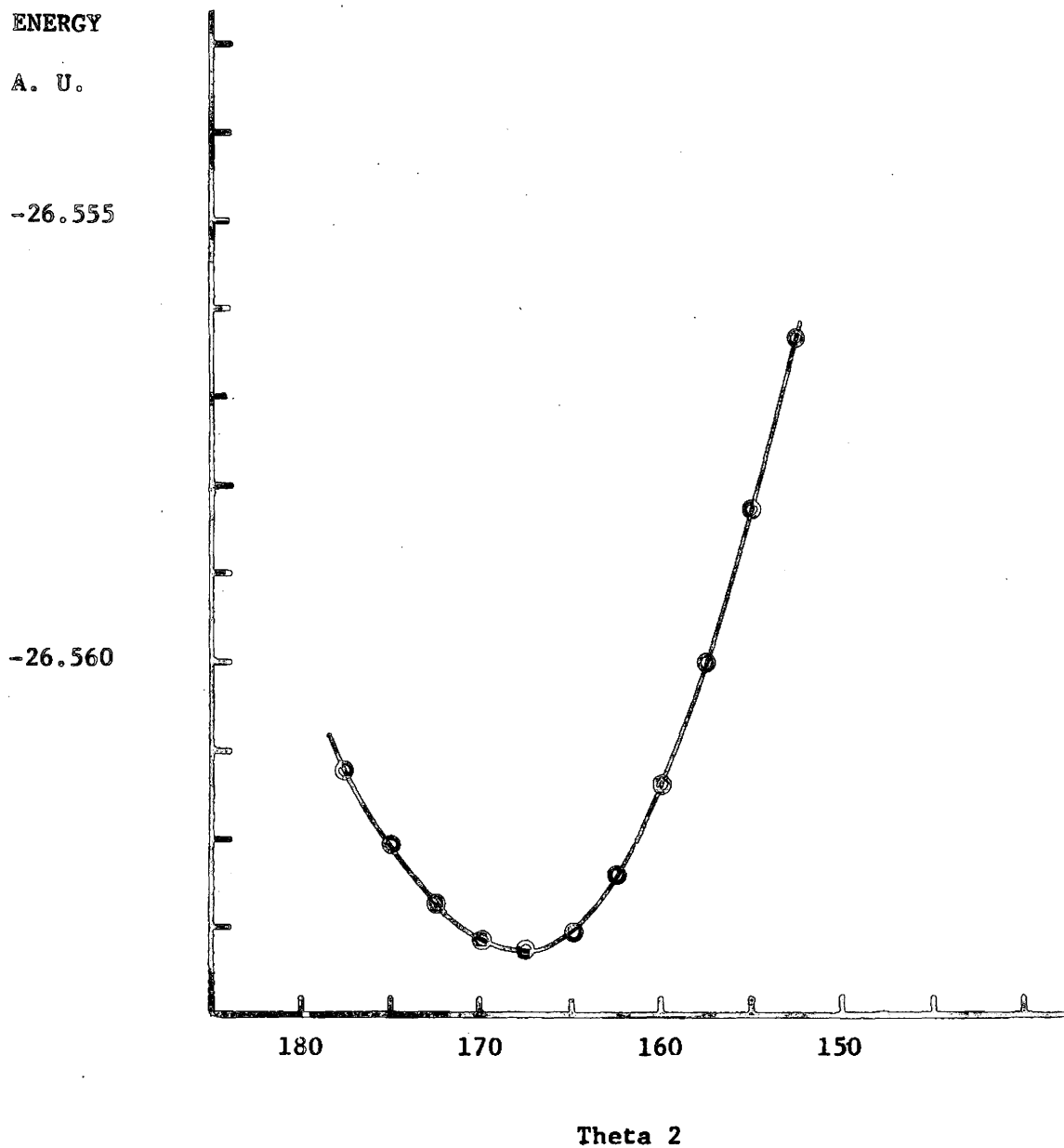
Figure XIV: Energy of HCO + H (Ground State) as a Function of Theta 2.



Coordinates:  $R_1 = 1.24 \text{ \AA}$ ;  $R_2 = 1.09 \text{ \AA}$ ; and,  $R_3 = 3.0 \text{ \AA}$ .

Theta 1 =  $46^\circ$

Figure XV: Energy of HCO + H (Ground State) as a Function of Theta 2.



Coordinates:  $R_1 = 1.24 \text{ \AA}$ ;  $R_2 = 1.09 \text{ \AA}$ ; and,  $R_3 = 2.5 \text{ \AA}$ .

Theta 1 =  $48^\circ$



the one correlating with these products. The situation is analogous to the one for the formation of the molecular products. The configuration  $\pi, \pi^*$  probably corresponds to some highly excited state of the product. As the two states travel the path to products they approach each other, and large mixing of configurations occur. The states will repel each other and the  ${}^3\pi, \pi^*$  state (properly designated as the  ${}^3A'$ ) will have a larger contribution from the  $n, \sigma^*$  configuration than its own original configuration. As a result, the configuration is more accurately described as  $n, \sigma^*$  than  $\pi, \pi^*$ .

If the reaction path is, in fact, non-planar, the correlation diagram will be modified to that in Fig. XIII B.

To summarize, the proposed correlation of states and products is as follows: the ground state correlates with the products  $H_2 + CO$ , in their ground states, the ground state and the  ${}^3\pi, \pi^*$  state correlate with the products  $HCO {}^2A'$  and  $H^2S_g$ , and the  ${}^1n, \sigma^*$  and  ${}^3n, \pi^*$  states correlate with the products  $HCO {}^2A''$  and  $H^2S_g$ . The configuration of the state leading to the products  $HCO {}^2A'$  and  $H^2S_g$  is probably  $n, \sigma^*$ .

Abrahmson, Littler, and Vo<sup>21</sup> propose that the state leading to  $H_2 + CO$  products in their ground states is  ${}^1n, \sigma^*_{CH_2}$ . This state is, in the  $C_{2v}$  point group  ${}^1B_2$ , and in non-planar  $C_s$  symmetry  ${}^1A''$ . The correlation, however, specifies that one  $b_2$  or  $a''$  orbital be doubly occupied, and one  $b_2$  ( $n$ ) or  $a''$  orbital be singly occupied. When the products arise, the  $b_2$  or  $a''$  orbitals correspond to one  $\pi$  bonding and  $\pi$  antibonding orbital on CO, and one  $\Sigma$  orbital on  $H_2$ . Thus, specifying these electrons among these three orbitals, one being doubly occupied, must result in an excited state of either CO or

$H_2$ . Also, as the symmetry is  $^1A''$ , it cannot correlate with products transforming as  $A_1$  or  $A'$ .

In the case of the radical products, Abrahamson et al suggest the  $^1_{n,\sigma^*}CH_2$  state as the one giving rise to the products  $HCO \ ^2A' + H \ ^2S_g$ . In  $C_s$  (planar) symmetry, the orbital  $\sigma^*_{CH_2}(a')$  cannot be specified as all the other  $\sigma^*$  orbitals become  $a'$ . Also, the interaction of states has not been considered, and it would be expected that the  $^1_{n,\sigma^*}$  state and the ground state will mix and thus "repel" each other. The  $^1_{n,\sigma^*}$  electronic configuration is probably close to that which gives rise to these products. However, configuration mixing will dictate the lowest  $^1A'$  state as the state giving rise to these products,  $HCO \ ^2A' + H \ ^2S_g$ , as these are the lowest products resulting from the split of one H atom from the formaldehyde molecule.

As discussed above, the excited state which smoothly correlates with the radical products, in the ground state, will be the  $^3_{\pi,\pi^*}$  state, a triplet state not a singlet state as proposed by Abrahamson et al. However, these products either may arise as a result of an internal conversion between the  $^3_{n,\pi^*}$  state ( $^3A''$ ) and the  $^3_{\pi,\pi^*}$  state ( $^3A'$ ), or may occur smoothly from the  $^3_{n,\pi^*}$  state via configuration mixing if the path has no symmetry.

#### A Photochemical Mechanism

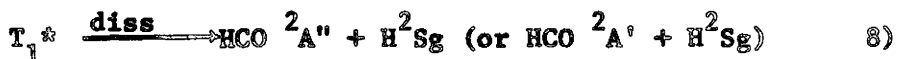
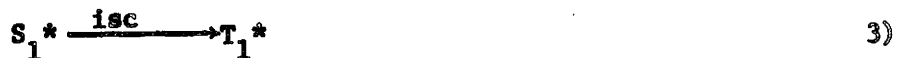
Upon excitation to a vibrationally excited level of the  $^1_{n,\sigma^*}$  state a number of possible processes can occur. The molecule may have sufficient energy to dissociate, resulting in the product  $HCO \ ^2A' + H \ ^2S_g$ , or it may intersystem cross to the triplet state, or finally the vibrational energy may be collisionally deactivated, the molecule then existing in the

low lying levels of the singlet state. There is also the possibility of fluorescence, but as this has not been observed for the upper vibrational levels of the  $^1_{n,\pi}$  state, it will not be considered.

If the molecule exists in the low lying vibrational levels of the first excited state it can undergo intersystem crossing to the triplet state, internal conversion to the high vibrational levels of the ground state or undergo fluorescence. Fluorescence will result in a molecule in the lower levels of the ground state, which will undergo no further processes of interest. The ground state formed by internal conversion, however, may have sufficient energy to decompose and will result in molecular products in their ground states.

The triplet state molecules,  $^3_{n,\pi^*}$ , may either decompose directly to products ( $\text{HCO } ^2A'' + \text{H}^2S_g$ ) or undergo decomposition through a path of  $C_1$  symmetry, resulting in the product  $\text{HCO } ^2A'$  and  $^2S_g$ . The latter is equivalent to intersystem crossing to the  $^3_{\pi,\pi^*}$  state, induced by the out of plane vibration. The triplet may also be deactivated to the ground vibrational levels of this state which can phosphoresce, intersystem cross to the ground state, or be collisionally reactivated to higher vibrational levels. Of these possibilities, emission will not be considered further as it has only been observed in low temperature matrices<sup>2</sup>.

The possible processes occurring upon excitation to the excited singlet  $^1_{n,\sigma^*}$  state are as follows:



F: the ground state of formaldehyde.

$S_1$ : The first excited singlet of formaldehyde.

$T_1$ : the first excited triplet of formaldehyde.

the superscript  $\circ$ : the low lying vibrational levels

of formaldehyde the superscript  $*$ : high vib. levels of formaldehyde.

Excitation by short wavelengths will result in

predominance of processes (2), (3), (8). At higher pressures, there will be some deactivation to the lower levels of S. However, at higher temperature ( $\rightarrow 100^\circ\text{C}$ ) process (11) will be fast, and radical products will again predominate. At lower energies, there will be an increase in the number of molecules existing in the low lying levels, resulting in an

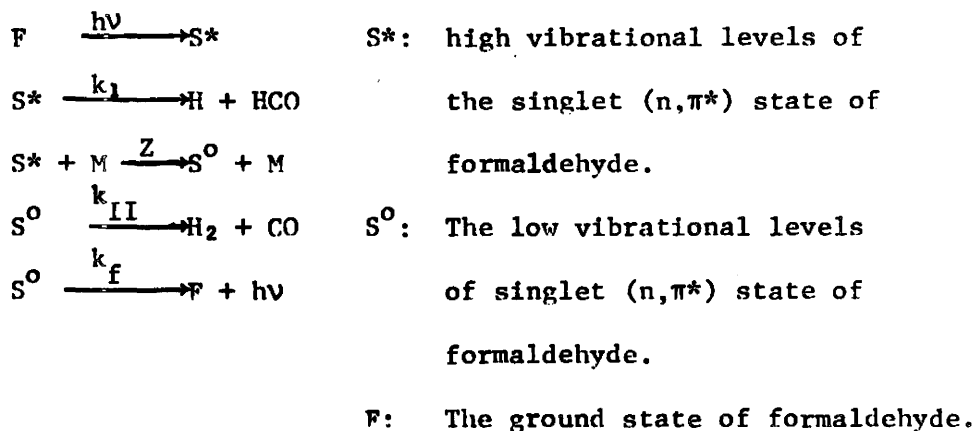
increase in molecular products. However, once again, this will be pressure dependant as, at elevated temperatures, the system will obey a Hinshelwood-Lindemann behaviour and radical products will predominate. Thus, the conditions favouring molecular products will be excitation in the long wavelength edge of the absorption band, and low pressures.

## Chapter IV

### Suggestions for Further Experiments

To determine whether such a mechanism involving thermally induced activation to higher vibrational levels is operative a study of the fluorescence quantum yield ( $\phi_f$ ) and the fluorescence lifetime ( $\tau_f$ ) should be made, as a function of pressure at 3655 nm and 100°C. This, coupled with a study of the decomposition yield of processes I and II as a function of pressure at this temperature, would show which of the processes, if any, is thermally excited to predissociative levels.

Further investigations should be carried out on the ratio  $\phi_I/\phi_{II}$  and the absolute values of these quantities as a function of pressure at various exciting wavelengths. If the thermal activation theory is correct, then, at high pressure, all rate constants would be independent of exciting wavelength and pressure. If, on the other hand, this theory is incorrect, then increasing the pressure will affect the values of  $\phi_f$  and  $\phi_{II}$  in the same manner such that a plot of  $\phi_f^{-1}$  or  $\phi_{II}^{-1}$  vs.  $p^{-1}$  will be linear. That is, assuming the following mechanism:



$$\text{then } \phi_{S^0} = \frac{Z[m]}{k_I + Z[m]}$$

$$\phi_f = \phi_{S^0} \frac{k_f}{k_{II} + k_f}$$

and as  $\phi_{S^0}$  is the only pressure dependent term,

$$\text{then } \frac{1}{\phi_f} = \left[ 1 + \frac{k_I}{Z} p^{-1} \right] \frac{k_{II} + k_f}{k_f}$$

and the plot  $\phi_f^{-1}$  vs  $p^{-1}$  would be linear. A similar relation for  $\phi_{II}$  would be true.

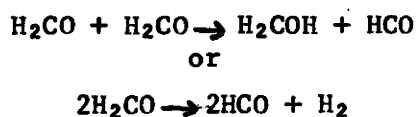
The extent of triplet participation in the photochemistry of formaldehyde is difficult to assess as there is no phosphorescence in the gas phase to monitor its presence. However, the quantum yield could be obtained by measuring the cis-trans isomerization of butene-2<sup>39</sup>. If any process should arise exclusively from the triplet state, the quantum yield of triplet, will be identical to the quantum yield of that process, for any given set of conditions.

Further, it is to be noted that the transition  $^3(\pi^*_{en})$  has a well resolved spectrum<sup>14,15,18</sup>. Thus, direct excitation of the triplet state is possible, and an evaluation of the role of the triplet state in the photochemistry can be greatly assisted by a study of the products of this reaction. Specifically, the absence of any product resulting from process II will be proof of the singlet being solely responsible.

Further studies monitoring the quantum yield of either process as a function of the pressure of known triplet quenchers, such as dienes or biacetyl would be useful. The studies with di-olefin, however, will be complicated by the fact that radical products, which arise from states not quenched by di-olefins, such as

singlets, will also be trapped. If, in fact, a di-olefin removes more of the radical products (process I) than, say, biacetyl, then the amount of radical products arising from a singlet state or a short-lived triplet state can be calculated.

Methods of determining the path leading to the molecular products, should they arise from the singlet state, are not straightforward. If these products predominate when excitation energy is low and possibility of thermal reactivation is low, then it is apparent that they do not arise from a decomposing singlet state. Similarly, it seems unreasonable to assume an intersystem crossing to a decomposing triplet. This suggests that they arise from the crossing to another state which is dissociative. Evidence other than the calculations above, that it may be the ground state, is not available as the products of thermal decomposition arise by virtue of a chain mechanism initiated by a disproportionation of two formaldehyde molecules rather than by a direct dissociation<sup>40</sup>. That is:





Chapter V

A Review of Experimental Information

The Spectroscopy and Photochemistry

The acetone photochemical system has received considerable attention from many researchers<sup>1,41-43</sup>. When acetone is excited to its lowest lying excited singlet state, the  $^1 n, \pi^*$  state, both luminescence and decomposition are observed. It is noted that although fine structure is observed in the absorption spectrum of acetone, illumination at all absorbing wavelength results in decomposition<sup>1</sup>. The spectrum of the luminescence occurs between 3800 nm and 4700 nm with a maximum at about 4500 nm for an excitation at 3130 nm<sup>1</sup>. The emission efficiencies are approximately  $2 \times 10^{-2}$ . The absorption spectrum of acetone has a long wavelength edge at approximately 3500 to 3600 nm. Thus, the 0-0 transition is not observed, nor is resonance fluorescence<sup>1</sup>.

A recent analysis of the absorption spectrum of acetone has been carried out<sup>45</sup> which indicates that acetone is bent, that is, the C-C-C skeleton is non-planar with a barrier to inversion of  $100 \text{ cm}^{-1}$ . CNDO II calculations showed that the out-of-plane angle is  $\approx 10^\circ$ <sup>45</sup>. This is compatible with the absence of a 0-0 transition, since the Frank-Condon factors are quite small. That resonance emission is not observed indicates that emission is taking place from the low lying levels of the upper state.

The luminescence consists of two distinct types: one

independent of pressure of known triplet quenchers; the other is the major portion, and can be quenched by molecules such as oxygen and olefins<sup>1,44,39,46</sup>. The quenchable emission, arising from the triplet state is classed as phosphorescence. It has a lifetime of about  $2 \times 10^{-4}$  secs<sup>42</sup>, and is about 90% of the emission<sup>44</sup> at 3130 nm. The non-quenchable part, ascribed to fluorescence from the singlet state, has a lifetime of about  $2 \times 10^{-9}$  secs<sup>47</sup>.

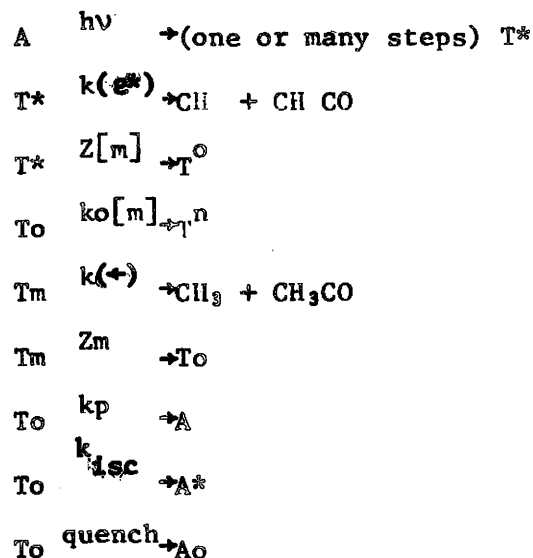
Heicklen<sup>44</sup> observed the ratio of fluorescence to phosphorescence  $\phi_f/\phi_p$  to be both wavelength and pressure dependent. The phosphorescence yield increased both with pressure and wavelength while the fluorescence yield remained relatively constant, although there is a noticeable, albeit slight, increase with wavelength. The quantum yield of emission, although weakly dependent on temperature, does decrease with temperature, and a negative activation energy of about 0.54 kcal/mole has been measured<sup>41</sup>.

Dissociation occurs at all absorbing wavelengths in the  $n,\pi^*$  system<sup>1</sup>. The products of this dissociation are  $\text{CH}_4$ ,  $\text{C}_2\text{H}_6$ , biacetyl and other high molecular weight alcohols and ketones in small quantities<sup>1</sup>. Excitation at 313 nm at temperatures above  $100^\circ$ , and excitation at short wavelengths, eg. 253.7 nm results mainly in methane, ethane, and carbon monoxide, the quantum yield of carbon monoxide being almost unity<sup>1,39</sup>. The primary dissociation has been shown to result in  $\text{CH}_3 + \text{CH}_3\text{CO}$  as the products. The acetyl radical then undergoes thermal decomposition or radical reaction. That the products are not  $2\text{CH}_3 + \text{CO}$  has been shown by iodine inhibition studies<sup>1</sup>. The same studies also showed that at elevated temperature or shorter wavelength, the  $\text{CH}_3\text{CO}$  does not dissociate immediately. It has been proposed

that, when the acetone decomposes, there is excess vibrational energy that can be divided between the acetyl and methyl radicals. Some acetyl radicals will have sufficient vibrational energy such that rapid dissociations can occur<sup>1</sup>.

While the nature of the products of the decomposition has been established, the nature of the states giving rise to these products and the mechanism by which these states undergo decomposition must also be considered.

Studies of the effect of triplet quenchers have shown that the quenching of products parallels the quenching of phosphorescence, that is, that the triplet state is responsible for a large portion of the decomposition<sup>1,41,44,39,46</sup>. There remains a portion of the decomposition products that is unquenchable. Some researchers ascribe this to decomposition from the singlet<sup>39</sup>, while others suggest that the decomposition results from highly vibrationally excited triplet states formed initially from the singlet<sup>41</sup>. Larson and O'Neil<sup>41</sup> propose the following mechanism:



That is, the decomposition of the triplet follows two paths, one in which the initially formed triplet is in some high vibrational level  $T^*$ , which can undergo decomposition in competition with deactivation to the ground levels of the triplet. The vibrationally equilibrated triplet,  $T^0$ , can then undergo a thermal unimolecular type decomposition in competition with quenching and emission as well as internal conversion to the ground state.

The manner in which the ground vibrational levels of the triplet state become populated will have no effect on the lifetime of these levels. Thus, a study of the phosphorescence lifetime will yield considerable insight into the mechanism removing the triplet. It is to be noted that, assuming an emission rate constant of approximately  $10^3 s^{-1}$ , emission from the vibrationally excited levels of the triplet will not compete with vibrational deactivation which has a rate constant of the order of  $10^9 M^{-1} s^{-1}$ .

Kaskan and Duncan<sup>42</sup>, in their study of the effect of pressure on the triplet lifetime, did not observe a Stern-Volmer relationship, but rather one of the form:

$$\tau^{-1} = k_1 + k_2 P / (1 + k_3 P)$$

$\tau$ : the lifetime

A steady state treatment of the above mechanism gives:

$$\begin{aligned} {}^3\tau^{-1} &= k_p + k_{ic} + {}^3kd \text{ (uni)} \\ &= \frac{(k_p + k_{ic}) + (k_p + k_{ic})[Z/k\epsilon] + k_o m}{1 + [Zm/kc]} \end{aligned}$$

If  $k_1 = (k_p + k_{ic})$ ;  $k_3 = Z/k\epsilon$ ;  $k_2 = [(k_1 + k_3) + k_o]$  the new equation of Larson and O'Neal reduces to a form similar to that

TABLE VII

Kinetic Data on Acetone by Larson & O'Neal<sup>41</sup>

RATE CONSTANT	VALUE
$3_{kd}$	$\frac{k_o k(\epsilon) M}{ZM + k(\epsilon)}$
$k_o$	$10^{9.81-5.95/\theta} M^{-1} S^{-1}*$
$k_{\infty} = \frac{k_o k(\epsilon)}{Z}$	$10^{10.14-9.6/\theta} M^{-1} S^{-1}$
$k_{ic}$	$10^{4.96-1.84/\theta} S^{-1}$
$k_T$	$10^{4.6-1.1/\theta} M^{-1} S^{-1}$

$$* \theta = 2.303 RT$$

## Unquenchable Decomposition

$k(\epsilon)*$	$A_{\infty}^* \left( \frac{E-E_c}{E} \right)^{S-1} S^{-1}$
$A_{\infty}^*$	$10^{11.1} S^{-1}$
$S$	5.7 - 7.6
$E_c$	9.1 - 10.3 Kcal/mole

originally proposed by Kaskan and Duncan. The data obtained from the lifetime and pressure studies of Kaskan and Duncan<sup>42</sup> and Groh Luckey and Noyes<sup>41,42,48</sup>, were treated by this mechanism, and their results are collected in Table VII.

The phosphorescence quantum yields of Heicklen<sup>44</sup> provide more evidence in favour of this type of scheme. The phosphorescence quantum yields show a marked effect of wavelength. If the triplet formed is of high energy, then the rate of decomposition will be much higher in relation to deactivation. Also, at short wavelengths a deactivating collision, which normally removes from 6-10 kcal/mole<sup>49</sup>, would bring the vibrationally excited species to a level which still was capable of dissociating, not to the ground level. The effect of pressure at any wavelength will be, in general, to increase the yield of ground vibrational triplet, which can then phosphoresce. However, an increase in pressure will also raise the unimolecular decomposition rate constant. Thus, at 3130nm an increase in pressure can reduce the quantum yield of phosphorescence.

This argument was tested on the phosphorescence data of Luckey and Noyes<sup>43</sup>. It can be shown<sup>41</sup> that the quantum yield of phosphorescence,  $\phi_p$ , in the scheme suggested by Larson and O'Neal will be:

$$Q_p = Q_{T^*} \left( \frac{Z_m}{k(e^*) + Z_m} \right) \left( \frac{k_p}{k_p + k_{ic} + {}^3k_{uni}} \right)$$

$Q_{T^*}$ , the quantum yield of triplets, will be close to unity, and will, therefore, be little affected by pressure. Substituting for  ${}^3k_{uni}$  and rearranging yields:

$$(Q_p F_m)^{-1} = \left( \frac{k_{ic} + k_p}{P_p} \right) + \frac{k_o}{k_p} \left( \frac{m}{X_m} \right)$$

$$F_m = 1 + \frac{k(\epsilon^*)}{Z_m}$$

$$X_m = 1 + \frac{m}{m_{1/2}}$$

$$\begin{aligned} m_{1/2} \text{ is the pressure at which } k_{\text{uni}} &= \frac{1}{2}k^\infty \\ &= \frac{k(\epsilon)}{Z} \\ &= \frac{k^\infty}{k_0} \end{aligned}$$

The plot of  $(O_p F_m)^{-1}$  vs  $\frac{m}{X_m}$  was linear.

The kinetics of the non-quenchable decomposition were considered<sup>41</sup> and the results are in Table I. The pre-exponential factors and activation energy are so close to those for the triplet decomposition that it is reasonable to ascribe residual decomposition to the vibrationally excited triplet.

The normal values of the pre-exponential factors for unimolecular decomposition are of the order of  $10^{13,50,51}$  while the pre-exponential factors for the acetone decomposition are of the order of  $10^{10}$ .

This low pre-exponential factor led Larson and O'Neal to state that the process occurs via a spin-forbidden triplet singlet conversion. However, if the transition to a repulsive singlet state takes place, it would seem even more likely the spin allowed transition to the corresponding triplet would take place, as the triplet would lie lower in energy. It is, in fact, difficult to make an assignment in this case as very little is known about the probability of these vibronic transitions. Until an accurate calculation of these probabilities of transition to either singlet or triplet is made, no more than tentative assignment of the state undergoing decomposi-

tion can be made.

Thus, while the experimental information concerning the decomposition of acetone is more detailed than that of formaldehyde, there remain many of the same problems, that is, the correlation of states with products, and the path taken as the molecule dissociates. The following study was undertaken to investigate these questions.



## Chapter VI

### Calculation on the Acetone System

The investigation of acetone was similar to that of formaldehyde. The size of acetone, both in terms of the size of the basis set and the large number of degrees of freedom, severely limited the number and type of calculation that could be carried out. Thus, only the ground state and some excited triplet states were investigated.

In the optimization of geometries, there are twenty-four dependent variables. The use of symmetry can reduce this somewhat, but a large number still remains. As a result, certain parameters were fixed at values corresponding to the average value found for similar types of molecules. The equilibrium geometry was chosen to be of  $C_{2v}$  symmetry, the C(CO)C skeleton planar with one hydrogen from each methyl lying in the plane, pointing towards the other (see Figure XV). The methyl hydrogens were assumed to have equivalent bond lengths and angles. The H-C-H angle was chosen as the tetrahedral angle,  $109^{\circ}27'$  and the H-C-C bond angle was also  $109^{\circ}27'$ . When the dissociation was investigated, the geometry of the methyl group was varied. The methyl was treated as a pyramid, the C-H bonds of equal length, and the C-C bond was perpendicular to the base. The geometry of the methyl group, then, is a function of  $\phi$ , the H-C-C bond angle.

The final assumption was that the C-H bond distance was fixed as  $1.09 \text{ \AA}$ . The two C-C bonds were considered equivalent, and the two C-C-O angles equal. Thus, the geometry can be specified by three parameters: the C-C-C bond angle,  $R_1$ , the C-O bond length and

$R_2$ , the C-C bond length. Unfortunately, this parameterization will introduce some inaccuracy into the calculated geometries.

### The Ground State and Excited State Geometries

The ground state of acetone, in  $C_{2v}$  symmetry, has the following molecular orbitals: nine  $a_1$  orbitals, seven  $b_2$  orbitals, four  $b_1$  orbitals, and, two  $a_2$  orbitals. The  $b_1$  and  $a_2$  orbitals are  $\pi$  type orbitals, that is, they receive contributions from only the  $p_z$  orbitals of carbon and oxygen, and the four out of plane hydrogen  $1s$  atomic orbitals, and therefore, have a node in the plane of the molecule.

The orbitals are occupied in the following order, two electrons in each orbital:  $1a_1$ ,  $2a_1$ ,  $1b_2$ ,  $3a_1$ ,  $1b_1$ ,  $2b_2$ ,  $4a_1$ ,  $1a_2$ ,  $3b_2$ ,  $5a_1$ ,  $2b_1$ ,  $4b_2$ . The lowest unoccupied orbitals are  $3b_1$  and  $6a_1$ .

The excited states were prepared by exciting an electron from the occupied orbitals  $4b_2$  or  $2b_1$  ( $n$  or  $\pi$ ) to the unoccupied orbitals  $3b_1$  or  $6a_1$  ( $\pi^*$  or  $\sigma^*$ ).

The equilibrium geometries were optimized by the same technique as was used in formaldehyde (see page 33) and the results of the calculations are collected in Table VIII.

### The Decomposition to Radical Products

The products of the decomposition of acetone are the methyl and acetyl radicals. The methyl radical is assumed formed in the ground state as its lowest lying excited state lies 5.7 eV above the ground state. The acetyl radical, however, is similar to the formyl radical in that there is a low lying excited state, so calculations were performed on the acetyl radical.

TABLE VIII

## Equilibrium Geometries of Various Electronic States of Acetone\*

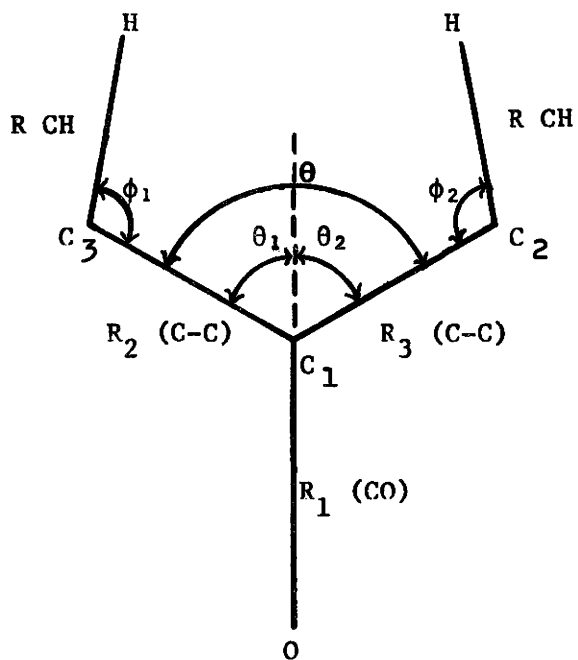
State	Geometries			Transitions ev	
	RCC Å	RCO Å	Theta	0-0	Vertical
GS	1.46	1.28	119°	--	--
<sup>3</sup> <sub>nπ*</sub>	1.47	1.33	126°	2.0	2.1
<sup>3</sup> <sub>ππ*</sub>	1.44	1.39	123°	3.4	3.7
<sup>3</sup> <sub>no*</sub>	1.52	1.32	162°	8.8	9.58
<sup>3</sup> <sub>π*</sub>	1.42	1.50	147°	10.0	11.59

All geometries assume  $R_{CH} = 1.09 \text{ Å}$ ,  $\angle HCH = 109^{\circ}27'$  and  $\angle H-CC = 109^{\circ}27'$  and  $C_{2v}$  symmetry.

\* The Coordinate System is in Figure XVI.

Figure XVI

The Coordinates Varied in the Calculations on Acetone



Acetyl, in the linear configuration, is a  ${}^2E$  state, belonging to the  $C_{3v}$  point group. This degenerate state is split by bending to a  ${}^2A'$  and  ${}^2A''$  state, the  ${}^2A'$  state having the lowest energy. The equilibrium geometries of these states were calculated, and are tabulated below (see Table IX). As the energies of these states are so close, they must both be considered as possible products.

The Wigner-Witmer rules, when applied to acetone give the same results as in formaldehyde (see Figure XIII). The methyl radical in the  $C_s$  point group is considered as  ${}^2A'$ . Thus, the ground state and  ${}^3\pi\pi^*$  states lead to the ground state products, while the two  $\eta\pi^*$  states correlate with the excited state products.

The  $\eta\pi^*$  state may cross to the  ${}^3\pi\pi^*$  surface via the out of plane vibration and will thus correlate with the ground state products. This is not unreasonable, as the molecule has been shown to be non-planar<sup>45</sup> in the  $\eta\pi^*$  state.

The most unambiguous means of determining the correlation of a set of electronic states with their products, and the geometry changes occurring as the molecule decomposes is to do a complete CI solution. However, it is to be noted that, as was stated above, when an electronic state is well separated from other interacting states, the mixing is very small. Thus, the single configuration wavefunction will not differ greatly from that of the CI wavefunction, and the behaviour will be expected to be similar. Some useful information can thus be found concerning the decomposition path of a molecule in a particular electronically excited state from a simple SCF calculation.

TABLE IX

The Equilibrium Geometries of Two States of Acetyl Radical

State	Geometry			Transition ev	
	RCO Å	RCC Å	Theta	O-0	Vertical
GS <sup>2</sup> A'	1.2	1.43	43°	--	--
<sup>2</sup> A''	1.2	1.4	0°	0.13	1.4

Assume the angle H-C-C = angle H-C-H = 109°27' and R C-H 109 Å.

As in the case of formaldehyde, it was found that the configuration  $^3 n, \sigma^*$  lead to the products HCO and H in their ground electronic states, the acetone  $^3 n, \sigma^*$  state was investigated as a possible source of radical products. This state was investigated at two methyl-carbon internuclear distance of the leaving methyl radical. These were 1.7 Å and 2.75 Å. As described above, the geometry of the methyl group was varied, and the two angles  $\theta_1$  and  $\theta_2$  were varied separately.

The angle  $\theta_2$  was optimized and found to be  $110^\circ$  for a C-CH<sub>3</sub> bond length of 1.7 Å. The other variables were then optimized and the angle  $\theta_2$  was reoptimized, and found to be  $114^\circ$  (see Figure XVII and Table X). The angle  $\phi$  is  $113^\circ$ , greater than the  $109^\circ 27'$  it was originally fixed at, and this is probably similar to the angle in the ground state.

A similar calculation was carried out for a C-CH<sub>3</sub> bond length of 2.75 Å, and the results are tabulated below (see Table IX). The angle  $\theta_2$  was found to be  $175^\circ$ , (see Figure XVIII), indicating that as the carbon-carbon bond stretches, the methyl group "rolls off" around the oxygen in a manner similar to the hydrogen atom in the decomposition of formaldehyde. The methyl group, as seen by a value for  $\phi$  of  $95^\circ$ , is approaching the planar geometry of the ground state methyl radical. The acetone geometry is approaching the geometry of the acetyl except the value of  $\theta_1$ , which is midway between the value for the excited and ground states of acetyl. This may be a result of incomplete optimization of all the variables.

### Discussion

The results of the calculations on acetone are similar to those done on formaldehyde. The  $^3 n, \sigma^*$  SCF state gives rise to

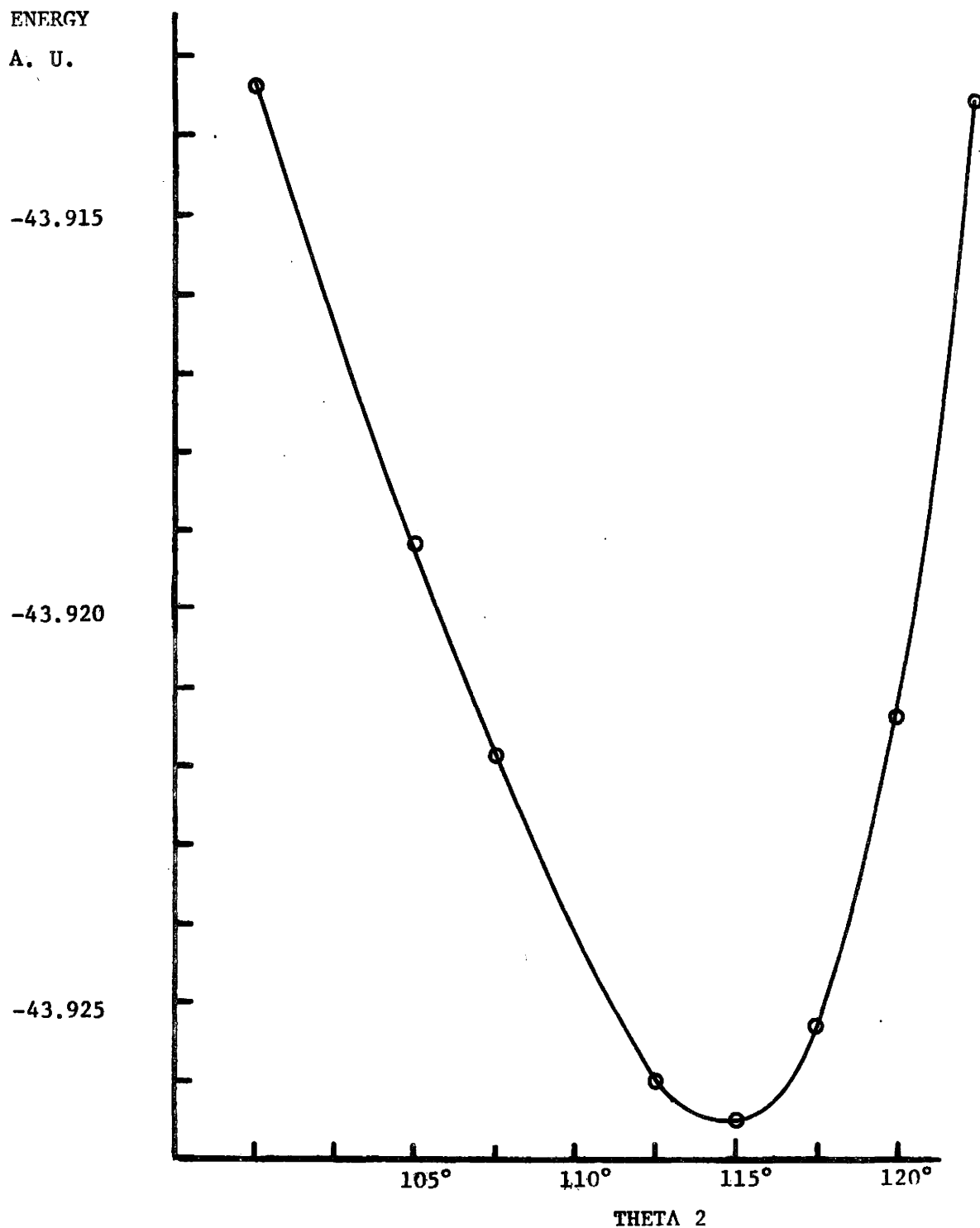


Figure XVII: Variation of the Energy of an Acetyl Radical with a Methyl radical: at a distance of 1.72 Å with the angle Theta 2.

Coordinates:  $R_1 = 1.28 \text{ \AA}$ ;  $R_2 = 1.44 \text{ \AA}$ ; and,  $R_3 = 1.72 \text{ \AA}$ . Phi:  $113.0^\circ$

Theta 1 =  $55^\circ$



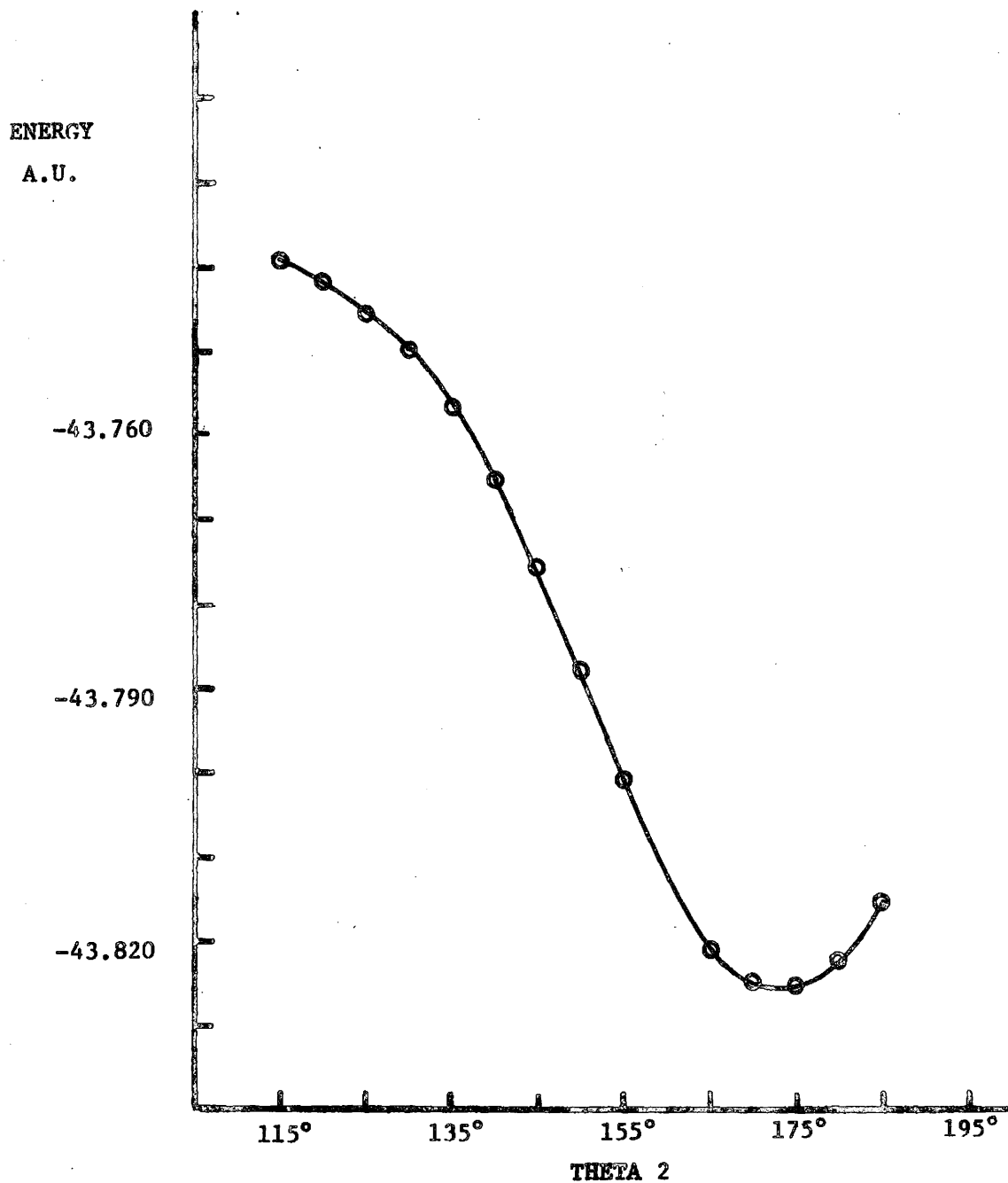


Figure XVIII: Variation of the Energy of an Acetyl Radical with a Methyl radical at a distance of 2.75 Å with the angle Theta 2.

Coordinates:  $R_1 = 1.25 \text{ \AA}$ ;  $R_2 = 1.44 \text{ \AA}$ ; and,  $R_3 = 2.75 \text{ \AA}$ . Phi:  $95^\circ$

Theta 1 =  $15^\circ$

TABLE X

The equilibrium geometries for values of  $R_3$  (C-C)  
of 1.7 Å and 2.75 Å

$R_3$ (C-C)	RCO	$R_2$ C-C	$\theta_1$	$\theta_2$	$\phi$
1.7 Å	1.28 Å	1.44 Å	55°	115°	113°
2.75 Å	1.25 Å	1.44 Å	15°	175°	95°

the ground state products,  ${}^2A'$   $\text{CH}_3\text{CO}$  and  ${}^2A'$ ( ${}^2A''$ )  $\text{CH}_3$ , and the leaving group "rolls off" around the oxygen atom. The Wigner-Witmer rules predict that the states giving rise to the ground state products are the ground state and  ${}^3\pi\pi^*$  state of acetone, while those giving rise to the excited state products,  ${}^2A''$   $\text{CH}_3\text{CO}$  and  ${}^2A'$ ( ${}^2A''$ )  $\text{CH}_3$ , are the two  $n\pi^*$  states (see Figure IV). The  ${}^3n,\pi^*$  state presumably internally converts to the  ${}^3\pi\pi^*$  via the out of plane vibration, or, if considered as going through a  $C_1$  symmetric transition state, then the Wigner-Witmer rules predict the  ${}^3\pi\pi^*$  state will correlate with the ground state products. However, the possibility remains that the  ${}^1n\pi^*$  state and  ${}^3n\pi^*$  state may dissociate directly to products which will be the excited state products.

As was mentioned above, there are at least two distinct paths for decomposition of the excited states of acetone, that which can be quenched by addition of olefins and other known triplet quenchers, ascribed to the triplet state, and a smaller unquenchable quantity. While the evidence is quite compelling in the former case, it is more difficult to determine the source of the latter. Larson and O'Neal<sup>41</sup> propose that this residual decomposition arises from a highly vibrationally excited  ${}^3n\pi^*$  first formed on intersystem crossing from the  ${}^1n\pi^*$  originally formed (see above) while Cundall and Davis<sup>39</sup> propose the  ${}^1n\pi^*$  as the source of this decomposition.

Both systems are, in fact, quite reasonable. However, if the singlet state is capable of decomposition, this does not mean the initially formed triplet cannot undergo decomposition in competition with vibrational equilibration. Both the singlet and the triplet can be responsible for the fraction of the decomposition to radical products

that is unquenchable by addition of known triplet quenchers, in normal amounts.

It has been found from iodine quenching studies that the product acetyl is formed in two distinct forms, one fraction having sufficient energy to decompose directly, the other fraction, the larger, capable of undergoing reactions before decomposition. The fraction of decomposing acetyl is 0.07 at 3130 nm and 0.22 at 2537 nm. It is possible that this may arise because some acetyl is formed as the  $^2A''$  excited state while the remainder as the  $^2A'$  state, the former decomposing more readily than the ground state. Alternatively, an acetyl  $^2A'$  formed in vibrationally excited state may decompose before being vibrationally equilibrated. The effect of wavelength on the quenchable acetyl is compatible with both postulates.

## CONCLUSION

### Chapter VI

#### Discussion

A number of electronic states of acetone, acetyl, formaldehyde, and formyl were investigated to determine their role in the photochemical process occurring upon excitation of the  $^1(\pi^* \leftarrow n)$  transition. The equilibrium geometries, 0-0 and vertical transitions were also determined, and good agreement was found with experimental data. Many of the states investigated have not been observed experimentally, and comparison was made with the results of calculations performed by other researchers. Good agreement, with a few exceptions, was obtained.

The study of the decomposition processes indicates that the process II decomposition of formaldehyde arises from the ground electronic state. This is predicted by the Wigner-Witmer rules, and the potential surface of the ground state shows, clearly, that it correlates smoothly to the ground state products  $H_2$  and  $CO$ . This process would occur, upon excitation to the singlet  $n, \pi^*$  state by an internal conversion from the singlet to high vibrational levels of the ground state. There is also the possibility of intersystem crossing from the triplet  $n, \pi^*$  state. The possibility of triplet involvement in this mode of decomposition could be investigated directly by a direct excitation to the triplet  $n, \pi^*$  state.

The behaviour of the decomposition of acetone and formaldehyde to radical products is quite similar. The Wigner-Witmer rules predict the same states giving rise to the radical products in their ground and final excited states. More detailed calculation, involving configuration interaction, should be made to determine the symmetry of the path followed,

as these excited states,  $^1,^3n,\pi^*$  and  $^3\pi,\pi^*$  states, decompose.

A possible mechanism has been proposed, one incorporating a Larson and O'Neal type mechanism for the triplet decomposition, which is the same for both acetone and formaldehyde. Excitation to the singlet state is followed by possible direct decomposition of the singlet state, vibrational equilibration to the low levels of the singlet, or intersystem crossing to the high levels of the triplet state. The vibrationally equilibrated singlet state can either intersystem cross to the triplet, internally convert to the ground state, in the high vibrational levels, or fluoresce. The triplet state, in the high vibrational levels, can decompose immediately, or be vibrationally deactivated to the low levels of the triplet state. This vibrationally equilibrated triplet can phosphoresce, be reactivated to the dissociative levels of the triplet, or intersystem cross to the ground state, in the high vibrational levels.

The mode of decomposition of the singlet and triplet state may be either direct decomposition, or crossing to the surface of the  $^3\pi,\pi^*$  state.

In the formaldehyde system, the internal conversion to the ground state results in molecular products. That there is internal conversion from the acetone  $^1n,\pi^*$  state to the ground state, is not known. Formaldehyde does not emit from the  $^3n,\pi^*$  state, in the gas phase, but as formaldehyde is a small molecule, spin-orbit coupling will not be very large and the rate constant for emission will be small compared to the rate of activation to excited levels. At low temperature, when thermal activation is not significant, formaldehyde does emit from the  $^3n,\pi^*$  state.

References

1. W. A. Noyes, Jr., G. B. Porter, and J. E. Jolley, *Chem. Rev.*, 56, 49 (1956).
2. R. B. Cundall and A. S. Davies, *Trans. Farad. Soc.*, 60, 1146 (1964).
3. J. N. Murrell, T. N. Kettle, and J. M. Tedder, "Valence Theory", John Wiley and Sons, Ltd., New York, 1965.
4. J. C. Slater, "Quantum Theory of Molecules and Solids, Vol. I: Electronic Structure of Molecules", McGraw-Hill, New York, 1963.
5. R. G. Parr, "Quantum Theory of Molecular Electronic Structure", W. A. Benjamin, New York, 1964.
6. F. G. Pilar, "Elementary Quantum Chemistry", McGraw-Hill, New York, 1968.
7. J. A. Pople and D. L. Beveridge, "Approximate Molecular Orbital Theory", McGraw-Hill, New York, 1970.
8. J. A. Pople, D. P. Santry and G. A. Segal, *J. Chem. Phys.*, 43, S129 (1965).
9. J. A. Pople and G. A. Segal, *J. Chem. Phys.*, 43, S136 (1965).
10. J. A. Pople and G. A. Segal, *J. Chem. Phys.*, 49, 3289 (1968).
11. C. C. J. Roothaan, *Rev. Mod. Phys.*, 23, 69 (1951).
12. C. C. J. Roothaan, *Rev. Mod. Phys.*, 32, 179 (1960).
13. J. A. Pople, *Proc. Roy. Soc.*, A68, 81 (1965).
14. J. C. D. Brand and R. I. Reed, *J. Chem. Soc.*, 23, 86 (1957).
15. V. E. DiGiorgio and G. W. Robinson, *Can. J. Chem.*, 36, 316 (1958).
16. B. DeGraff and J. G. Calvert, *J. Amer. Chem. Soc.*, 89, 2247 (1967).

17. J. J. Smith and B. Meyer, J. Chem. Phys., 50, 456 (1969).
18. G. Herzberg, "Molecular Spectra and Molecular Structure, Vol. III: Electronic Spectra and Electronic Structure of Polyatomic Molecules", D. Van Nostrand, Princeton, 1966.
19. G. W. King, "Spectroscopy and Molecular Structure", Holt, Rinehart and Winston, New York, 1964.
20. J. C. D. Brand, J. Chem. Soc., 858 (1950).
21. E. W. A. Grahamson, J. G. F. Little and K. P. Vo, J. Chem. Phys., 44, 4082 (1965).
22. K. Sukarai, G. Capelle, and H. P. Broida, J. Chem. Phys., 54, 1412 (1971).
23. E. S. Yeung and C. B. Moore, J. Amer. Chem. Soc., 93, 2059 (1971).
24. J. G. Calvert and S. N. Pitts, Jr., "Photochemistry", John Wiley and Sons, New York, 1966.
25. M. Jeunehomme and A. B. F. Duncan, J. Chem. Phys., 41, 1692 (1963).
26. M. Venogopulan and K. O. Kutschke, Can. J. Chem., 42, 2451 (1964).
27. R. Klein and L. J. Schoen, J. Chem. Phys., 7, 256 (1939).
28. E. Gorin, J. Chem. Phys., 256 (1939).
29. R. M. McGuigg and J. G. Calvert, J. Amer. Chem. Soc., 88, 4570 (1966).
30. E. Murad and M. G. Imghram, J. Chem. Phys., 41, 404 (1964).
31. R. Walsh and S. W. Benson, J. Amer. Chem. Soc., 88, 4570 (1966).
32. H. W. Kroto and D. P. Santry, J. Chem. Phys., 47, 2736 (1967).
33. A. J. Beunker and S. D. Peyerimhoff, J. Chem. Phys., 1368 (1970).



34. A. D. Buckingham and J. T. Tyrell, *Can. J. Phys.*, 48, 1242 (1928).
35. A. N. Bene and L. O. Jaffe, *J. Chem. Phys.*, 50, 1126 (1969).
36. C. Gulesner-Pretre and A. Pullman, *Theoret. Chim. Acta*, 17, 120 (1970).
37. G. Segal, *J. Chem. Phys.*, 53, 360 (1970).
38. J. L. Whitten and M. Hackmeyer, *J. Chem. Phys.*, 51, 5584 (1969).
39. R. B. Cundall and A. S. Davies, *Proc. Roy. Soc. (London)*, A290, 563 (1966).
40. I. D. Gay, G. P. Glass, G. B. Kistiakowsky and H. Niki, *J. Chem. Phys.*, 43, 4017 (1965).
41. C. W. Larson and H. E. O'Neal, *J. Chem. Phys.*, 73, 1011 (1969).
42. W. E. Kaskan and A. B. F. Duncan, *J. Chem. Phys.*, 18, 427 (1950).
43. G. W. Luckey and W. A. Noyes, *J. Chem. Phys.*, 19, 227 (1951).
44. J. Heicklen, *J. Amer. Chem. Soc.*, 81, 3863 (1959).
45. C. N. Rao, G. C. Chaturvedi and H. Rhondawa, *J. Chem. Phys. Lett.*, 7, 563 (1970).
46. J. Heicklen and W. A. Noyes, Jr., *J. Amer. Chem. Soc.*, 81, 3858 (1959).
47. R. F. Borkman and D. R. Kevins, *J. Chem. Phys.*, 44, 945 (1966).
48. H. Groh, G. W. Luckey and W. A. Noyes, *J. Chem. Phys.*, 21, 115 (1953).
49. I. Amdar and G. G. Hammes, "Chemical Kinetics: Principles and Selected Topics", McGraw-Hill, New York, 1966.
50. J. W. Simmons, R. S. Rabinovitch, and D. W. Setser, *J. Chem. Phys.*, 41, 800 (1964); *ibid.* 40, 1751 (1964).

51. K. J. Laidler, "Chemical Kinetics", 2nd Ed., McGraw-Hill, New York, 1965.

**APPENDIX**

TABLE XI

The Eigenvectors of Formaldehyde in the Ground Electronic State, at Equilibrium Geometry

		Virtual Orbitals					
Symmetry		5a <sub>1</sub>	3b <sub>2</sub>	4a <sub>1</sub>	2b <sub>1</sub>		
Atomic Orbitals	H1S	-.115766	-.461998	.512785	.000000		
	H1S	-.115766	.461998	.512785	-.000000		
	C2S	-.274946	.000000	-.619344	.000000		
	O2S	.363587	-.000000	.070498	-.000000		
	C2P	.000000	.729042	.000000	-.000000		
	O2P <sup>x</sup>	-.000000	-.203993	-.000000	-.000000		
	C2P <sup>x</sup>	.691818	.000000	-.240467	-.000000		
	O2P <sup>y</sup>	.535531	-.000000	.166501	.000000		
	C2P <sup>y</sup>	.000000	-.000000	-.000000	-.764219		
	O2P <sup>z</sup>	.000000	.000000	.000000	.644957		
	Symmetry		2b <sub>2</sub>	1b <sub>1</sub>	3a <sub>1</sub>	1b <sub>2</sub>	2a <sub>1</sub>
Atomic Orbitals	H1S	.402086	-.000000	.199794	-.353389	-.403539	-.144528
	H1S	.402086	.000000	.199794	.353389	-.403539	-.144528
	C2S	-.000000	-.000000	-.031423	.000000	-.548683	-.488649
	O2S	.000000	-.000000	.300870	-.000000	.412216	-.776138
	C2P	.294721	-.000000	-.000000	-.617768	-.000000	.000000
	O2P <sup>x</sup>	-.767980	.000000	-.000000	-.607120	.000000	-.000000
	C2P <sup>x</sup>	.000000	-.000000	.490078	-.000000	-.367733	.296917
	O2P <sup>y</sup>	-.000000	.000000	-.767123	.000000	-.260979	-.169988
	C2P <sup>y</sup>	-.000000	.644957	-.000000	-.000000	.000000	-.000000
	O2P <sup>z</sup>	.000000	.764219	.000000	-.000000	.000000	.000000

TABLE XI

The Eigenvectors of Formaldehyde in the Ground State at Equilibrium Geometry

$a_1^*$	$b_2^*$	$c_1^*$	$a_1^*$	$a_2^*$	$b_2^*$	$a_1^*$	$b_2^*$	$a_1^*$	Symmetry
.055728	-.126007	.000000	.008060	.000000	.261919	-.496509	-.412343	.035156	Atomic Orbitals H1S
-.041194	-.005605	-.284062	-.192122	.352826	.292812	.007537	-.204960	.305082	
-.041194	-.005605	.284062	-.192121	-.352827	-.292812	.007537	-.204960	.305082	
.055728	.126007	.000000	.008060	-.000000	-.261919	-.496509	.412343	.035156	
-.041194	.005605	-.284062	-.192121	.352826	.292812	.007537	.204960	.305082	C2S
-.041194	.005605	.284062	-.192122	-.352826	-.292812	.007537	-.204960	.305082	
-.068934	.200651	-.000000	-.021931	-.000000	.089439	.189240	-.436633	-.453487	
-.191344	.000000	.000000	.590356	.000001	-.000000	.013699	.000000	.322147	
.068934	-.200651	-.000000	-.021931	.000000	.089439	.189240	.436633	-.453487	O2S
.334535	.000000	-.000000	-.115961	-.000000	.000000	.076635	-.000000	-.009673	
-.184446	.285269	-.000000	-.454040	-.000000	.391842	.022964	.049660	.034752	C2P <sub>x</sub>
-.000000	.697868	-.000000	.000000	.000000	.097327	-.000000	-.131742	-.000000	
.184446	.285269	.000000	.454040	.000001	.391842	-.022964	.049660	-.034752	O2P <sub>x</sub>
-.000000	-.136735	.000000	-.000000	-.000000	-.040531	-.000000	.049916	.000000	
-.079546	-.331004	.000000	.071079	.000000	.304669	.447056	-.207166	.201863	C2P <sub>y</sub>
.693852	.000000	.000000	.114856	.000000	-.000000	.100117	.000000	.158547	
-.079546	.331004	-.000000	-.071079	.000000	-.304670	.447056	.207166	-.201863	O2P <sub>y</sub>
.516569	.000000	-.000000	-.231724	-.000000	.000000	.135089	-.000000	-.031683	
.000000	.000000	.482978	-.000001	.501026	.000000	.000000	-.000000	.000000	C2P <sub>z</sub>
-.000000	-.000000	-.408216	.000000	-.000000	-.000000	.000000	-.000000	.000000	
.000000	.000000	.482978	.000000	.501026	.000000	.000000	.000000	-.000000	O2P <sub>z</sub>
-.000000	.000000	.209902	-.000000	.000000	-.000000	-.000000	.000000	-.000000	

\* see note on page 103

TABLE XII (Continued)

$a_2^*$	$b_2$	$b_1$	$a_1$	$b_2$	$a_2$	$a_1$	$b_2$	$b_1$	Symmetry
.000000	.011640	.000000	.301253	-.343459	-.000000	.285762	-.309214	.000000	Atomic Orbitals
-.230345	.080590	-.214000	-.076832	.220287	.354279	-.159897	-.070199	.265432	
.230345	.080590	.214000	-.076832	.220287	-.354279	-.159897	-.070199	.265432	
.000000	-.011640	.000000	.301253	.343459	.000000	.285762	.309214	-.000000	
-.230345	-.080590	-.214000	-.076832	-.220287	-.354279	-.159897	.070199	.265432	1S
.230345	.080590	.214000	-.076832	-.220287	.354279	-.159897	.070199	-.265432	
-.000000	.111366	.000000	-.037991	.025139	.000000	-.030506	.122706	.000000	C2S
-.000000	.000000	.000000	-.010035	-.000000	-.000000	-.139365	-.000000	-.000000	
.000000	-.111366	-.000000	-.037991	-.025139	-.000000	-.030506	-.122706	.000000	O2S
.000000	.000000	.000000	-.146658	.000000	.000000	.403199	-.000000	.000000	
.000000	.330114	-.000000	-.073207	.340196	.000000	.193614	-.188962	-.000000	C2P <sub>x</sub>
-.000000	-.314837	.000000	.000000	-.196683	-.000000	.000000	.410645	.000000	
.000000	.330114	-.000000	.073207	.340196	.000000	-.193614	-.188962	.000000	O2P <sub>x</sub>
.000000	.767765	.000000	.000000	-.350033	-.000000	.000000	.480021	-.000000	
-.000000	-.145619	-.000000	.325291	.296671	.000000	-.339938	.374843	.000000	C2P <sub>y</sub>
-.000000	.000000	.000000	-.422929	-.000000	.000000	.196046	-.000000	.000000	
-.000000	.145619	.000000	.325291	-.296671	-.000000	.339938	-.374843	.000000	O2P <sub>y</sub>
-.000000	.000000	.000000	.607593	-.000000	-.000000	-.453912	.000000	-.000000	
.129220	.000000	-.228571	.000000	.000000	-.498972	.000000	-.000000	.444735	C2P <sub>z</sub>
.651695	.000000	.428636	.000000	.000000	.000000	.000000	.000000	.474262	
.129220	-.000000	-.228571	.000000	-.000000	.498972	.000000	-.000000	.444735	O2P <sub>z</sub>
-.574162	-.000000	.727048	.000000	.000000	.000000	.000000	.000000	.312538	

TABLE XII (Continued)

$a_1$	$b_2$	$a_1$	$a_1$	Symmetry
-.098924	.178277	-.232520	.113170	H1S
-.239670	.249544	-.122101	.120166	
-.239670	.249544	-.122101	.120166	
-.098924	-.178277	-.232520	.113170	
-.239670	-.249544	-.122101	.120166	
-.239670	-.249544	-.122101	.120166	
-.173961	-.482701	-.350322	.312959	C2S
-.394242	-.000000	-.078436	.574281	
-.173961	.482701	-.350322	.312959	O2S
-.212369	.000000	.576602	.554097	C2P <sub>x</sub>
.439737	.046902	-.090926	.116662	
.000000	.415823	.000000	.000000	O2P <sub>x</sub>
-.439737	.046902	.090926	-.116662	
.000000	.186449	.000000	-.000000	C2P <sub>y</sub>
-.093521	.070492	-.103144	-.085180	
.172016	.000000	-.457448	-.118595	O2P <sub>y</sub>
-.093521	-.070492	-.103144	-.085180	
.236202	-.000000	.033000	.167694	C2P <sub>z</sub>
.000000	-.000000	.000000	.000000	
.000000	-.000000	-.000000	-.000000	O2P <sub>z</sub>
.000000	-.000000	-.000000	.000000	
.000000	-.000000	.000000	.000000	

NOTE: The Starred Orbitals are the unoccupied (Virtual) Orbitals.

The H's are in two groups of three, in the following order: in plane; above plane; and, below plane. The first group is associated with  $C_3$ , the second with  $C_2$ . The carbons are in the following order:  $C_2$ ;  $C_1$ ; and,  $C_3$ . (See Figure XVI.)